NASA Contractor Report 170392

NASA-CR-170392-VOL-1
19830005836

NASTRAN MODEL OF A LARGE FLEXIBLE SWING-WING BOMBER

Volume I: NASTRAN Model Plans

W. D. Mock

September 1982

NASA
National Aeronautics and
Space Administration

NASA Contractor Report 170392

NASTRAN MODEL OF A LARGE FLEXIBLE SWING-WING BOMBER

Volume I: NASTRAN Model Plans

W. D. Mock
Rockwell International
Los Angeles Division
Los Angeles, California

Prepared for Dryden Flight Research Facility
under Contract NAS4-2308

National Aeronautics and
Space Administration
1982

TABLE OF CONTENTS

LIST OF ILLUSTRATIONS

LIST OF TABLES

NASTRAN MODEL OF A LARGE FLEXIBLE SWING-WING BOMBER

Volume I: NASTRAN Model Plans

W. D. Mock
Rockwell International Corporation
Los Angeles, California

SUMMARY

This report describes the preliminary development of a NASTRAN model of the B-1 aircraft No. 2 (A/C-2). The NASTRAN model is being developed as part of the airloads research study (ARS). The basic intent of the overall program is to utilize flight data acquired during B-1 flights, perform analyses of these data beyond the scope of Air Force requirements, and prepare research reports that will add to the technology base for future transport aircraft. Efforts are scheduled in distinct tasks with separate reports for each task.

During this contract phase, a review was conducted of A/C-2 internal loads models to determine the minimum model complexity necessary to fulfill all of the airloads research study objectives. Typical model sizings were tabulated at selected vehicle locations, and scale layouts were prepared of the NASTRAN structural analysis model. The structural stiffness data, mass properties data, and NASTRAN model layouts are included in the reference reports, rather than in this document.

INTRODUCTION

A/C-2 (figure 1) is being employed in the airloads survey flight test program. This aircraft has undergone extensive ground testing to calibrate the strain gages utilized in the airloads survey. The aircraft provides a reasonable simulation of a future transport aircraft since it employs the large flexible structure (figure 2) envisioned in future transport designs. The task described in this report is part of the ARS.

The airloads data gathered during the flight test program can be utilized in the evaluation of NASA computer programs recently developed to enhance the analytical techniques of predicting aeroelastic response of large flexible aircraft. These analytical techniques include computerized structural analysis programs such as NASTRAN and FLEXSTAB.

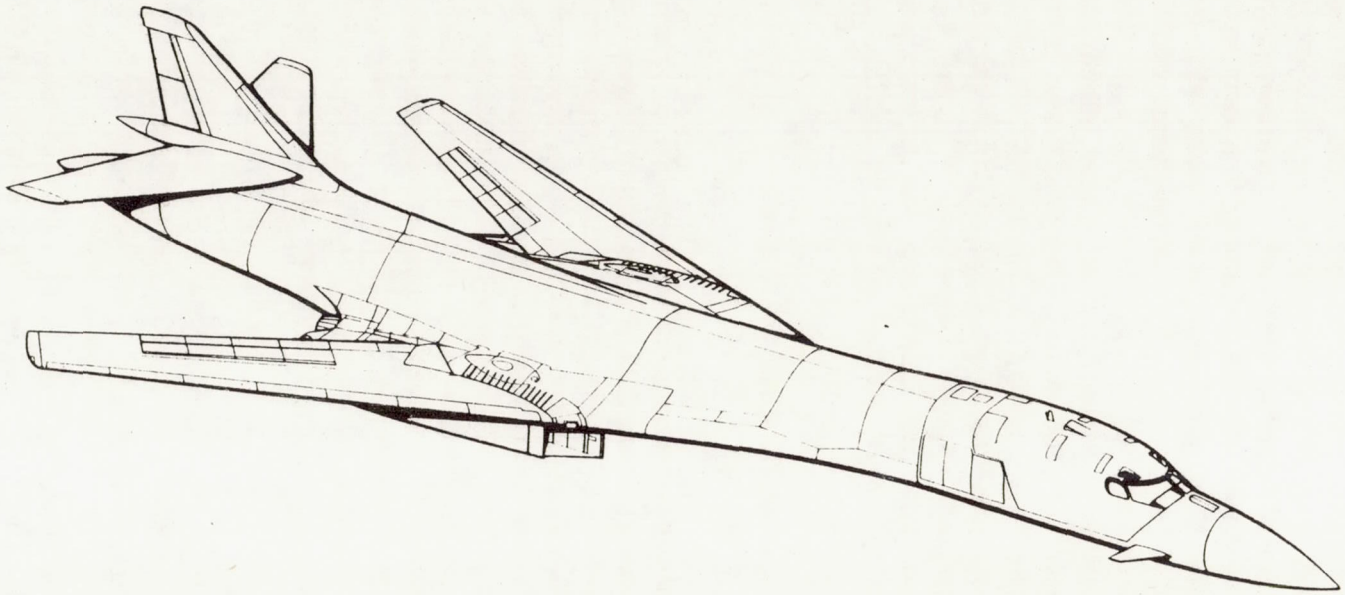

Figure 1.- B-1 aircraft.

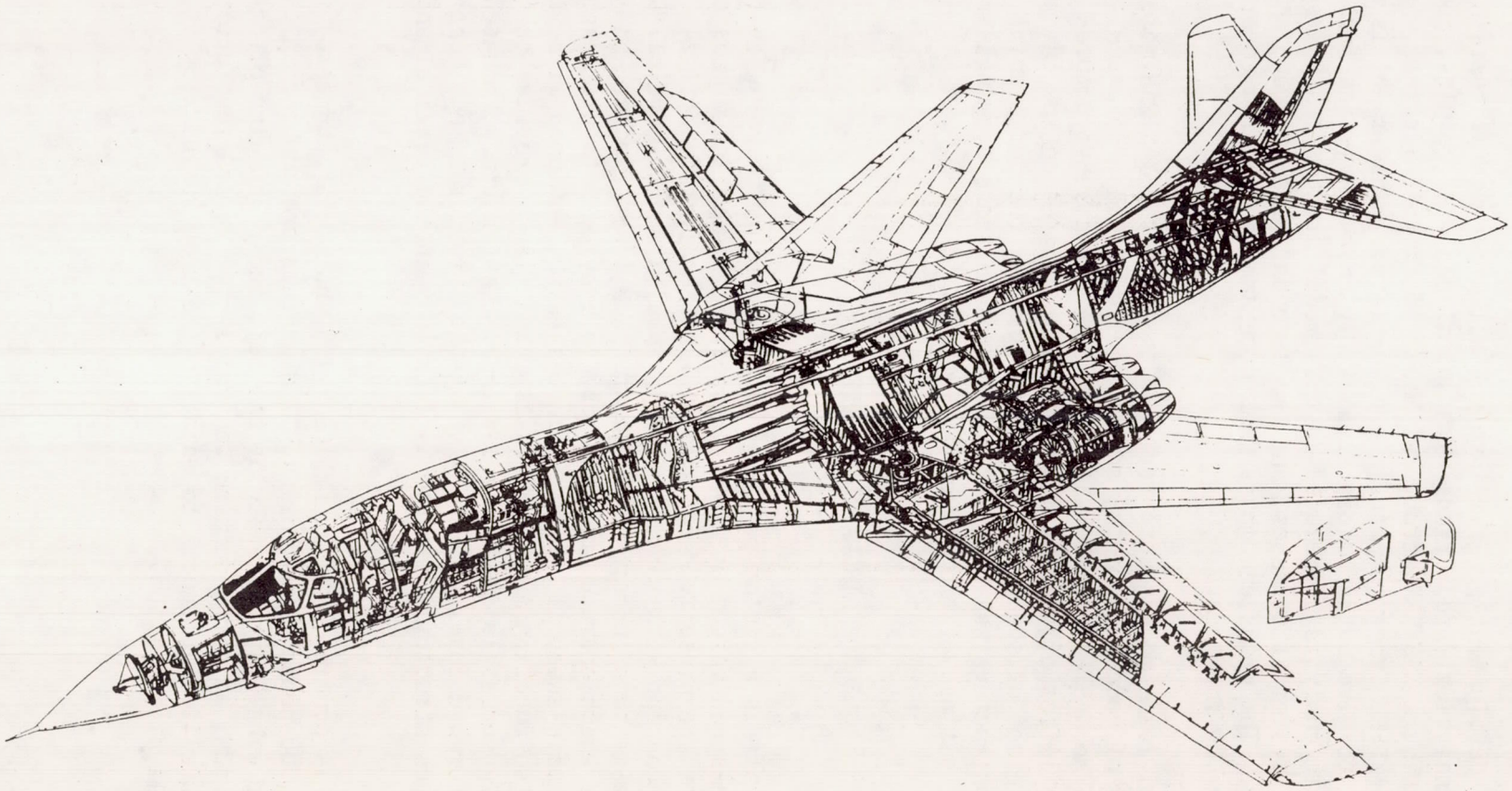

Figure 2.- Structural breakdown.

Since the B-1 development program involves all experimental tests needed to correlate the analytical predictions with actual measured results, detailed plans for constructing a NASTRAN structural model of the B-1 airframe, suitable for use on the NASA/DFRC Cyber computer, were initiated. This model is of minimum complexity to give satisfactory flexibility characteristics for FLEXSTAB aeroelastic analysis. Included in this model are the control surfaces, the control system stiffnesses, and the secondary loading edge and trailing edge structure. The plans encompass DMAP programming required to produce FLEXSTAB level 1.02.00 input data.

A/C-2 internal loads models were reviewed to scope the NASTRAN model to the minimum number of nodes, elements, and degrees of freedom for each structural component. The NASTRAN model will consist of seven substructures which will provide capabilities of instituting structural changes on any one structural component. A set of scaled model layouts showing the nodal point locations for each substructure was prepared. Included in these drawings are typical structural sizings of the structure employed in A/C-2.

AIRCRAFT DESCRIPTION

The B-1 aircraft is a prototype long-range supersonic bomber with the capability of high-speed flight at low altitude. Configuration dimensions and general arrangement are presented in figure A-1. The aircraft utilizes a blended wing-body concept with variable-sweep wings, a single vertical stabilizer with a three-section (upper, intermediate, and lower) rudder, and horizontal stabilizers which operate independently to provide both pitch and roll control. The variable-sweep (15 to 67.5 degrees) wing, equipped with slats, spoilers (which also function as speed brakes), and flaps, provides the aircraft with a highly versatile operating envelope. Canted vanes, mounted on each side of the forward fuselage, are part of the structural mode control system which reduces structural bending oscillations in the vertical and lateral axes.

The aircraft is powered by four YF101-GE-100 dual-rotor augmented turbofan engines in the 30,000-pound-thrust class. The engines are mounted in twin nacelles below the wing, approximately at the left and right wing pivot points. For supersonic speeds, an air induction control system varies the internal geometry of the nacelle inlet ducts to maintain the required airflow to the engines for all flight conditions.

Fuel is carried in integral tanks in the fuselage, wing carry-through, and wing outer panels. The fuel system is pressurized and inerted by nitrogen. Fuel transfer sequencing is automatic and provides center-of-gravity control. The aircraft has both in-flight and single-point refueling capabilities.

Fuselage

The fuselage (figure A-2) is constructed primarily of aluminum alloy materials arranged in a semimonocoque skin-frame-longeron type of construction. Titanium is used in the wing carry-through structure, in the nacelle and tail support structure, for various other structures where high load concentrations exist, and on aft fuselage skins where high temperatures and acoustic levels are prevalent. Dielectric materials such as polyimide quartz and fiberglass are used for radomes and antenna covers.

The fuselage structure is fabricated in six major sections and then mated together prior to attaching wings, empennage, landing gears, and nacelles. The following functional description of each section will provide a better understanding of the overall fuselage and its relationship to most of the aircraft subsystems.

The crew module assembly provides a sealed enclosure with crewmember provisions and is an ejectable unit for emergency escape. The structure is capable of pressurization for a 2439-meter (8000 feet) altitude environment and incorporates a clear-vision windshield designed to bird-proof requirements, additional crew windows, an entry door, and an emergency exit hatch for ingress and egress. The floor structure supports crew seating and ejection rocket loads. An unpressurized section aft of the crew quarters houses the escape system parachutes and provides support for the stabilizing fins. Two sets of deployable mechanical stabilizing spoilers are hinged in the side panel framework and at the lower forward edge of the module. Structural ties to the forward fuselage are severed by explosive charges for emergency escape.

The forward fuselage section includes the nose radome, a forward avionics compartment, an in-flight refueling receptable, the nose gear well and support structure, a central avionics compartment, a section of the forward fuel tank, a Doppler radome, an environmental control system equipment bay, and the crew entry stairladder structure and mechanism installation. The section also includes many other items of equipment such as antennas and pressure sensing devices. Left and right structural mode control fin surfaces are mounted on this section. Many large and small access doors are provided due to the high density of equipment installations in this assembly.

The forward intermediate section houses the forward and center weapons bays. Major bulkheads between the two bays and at each end of the bays provide support for the rotary weapons launchers. The aft bulkhead location also forms a part of the wing carry-through section. The forward bulkhead is also a closeout for the forward fuselage section. Large integral fuel tanks are incorporated into the forward intermediate fuselage structure, immediately outboard of the weapons bays. A systems routing tunnel occupies the upper structure area between longerons. Provisions for avionics are incorporated in the side fairing area, consisting of equipment bays, antennas, and radomes. Provisions for external stores pylons, wing sweep actuation components, and flap and slat drive mechanisms are also incorporated in the forward intermediate fuselage section.

The aft intermediate fuselage consists of the main gear well and the aft weapons bay. It incorporates a flight controls mixer compartment and a fuel tank above the main gear well. The gear uplock support structure is in the mixer compartment. Avionics provisions are made in the compartment between the wheel wells and in the structural compartments outboard of the wheels. Bulkheads at the forward and aft ends of the weapons bay support the weapons bay rotary weapons launcher. As in the forward intermediate fuselage, fuel is stored outboard of the weapons bay. A double-support frame for the aft portion of the nacelle extends outboard to the centerline beam of the nacelle. This support is approximately midway between weapons bay bulkheads. The upper centerline longeron and the lower outboard longerons are located and constructed so as to provide a high stiffness-to-weight ratio. The upper centerline longeron extends forward into the wing carry-through section and aft to the vertical stabilizer front spar.

The aft fuselage is a semimonocoque structure and consists of the aft fuel tank area, the dorsal area, the aft avionics bay, and the tail cone. The tank area is closed in the forward and aft ends by bulkheads. The forward bulkhead separates the aft fuel tank from the aft weapons bay. The aft bulkhead closes the tank and provides mounting support structure for the horizontal tail spindle fitting and the aft avionics bay. The dorsal area is a dry tunnel space which houses flight control cables and hardware and provides for the routing of the electrical conduits.

Wing

The wing consists of the wing pivot, outer wing panel, flaps, slats, and spoilers (figure A-3). The wing pivot consists of the pin, bearings, and inboard and outboard lugs, with provisions for attachment to the wing carry-through fuselage section and the wing outer panel.

The wing outer panel consists of a structural box with leading edge slats, trailing edge flaps, and spoilers over the flap leading edge. The outer wing is mounted on pivot bearings whose supporting lugs are mechanically attached to the wing covers. Provisions for integral fuel containment is provided in the outboard wing structural box. Access is provided for sealing, inspection, servicing, and replacement of fuel system components. Control surfaces on the wing include flaps, slats, and spoilers.

The flaps are aft of the wing rear spar and are mounted on rollers between curved tracks. Flap actuating jackscrews are in the mid bay of the flap panels. Segmented leading edge slats are provided. Each segment is supported on tracks mounted on rollers attached to the fixed leading edge structure. Segmented wing spoilers are aft of the wing rear spar and above the flaps.

Nacelle

The nacelle is constructed of aluminum alloy, titanium alloy, and stainless steel and fiberglass laminates. Structural type is semimonocoque with skins, frames, longerons, and a honeycomb sandwich duct (figure A-4). Each nacelle is fabricated in two major sections, the forward section and the engine compartment.

The forward section consists of the inlet section, the duct assembly, the ramps, and the center beam. The inlet section consists of the center splitter wedge and the upper and lower leading edges. Portions of the upper and lower leading edges are porous for boundary layer control. The duct assemblies consist of engine air intake ducts supported by frames and stringers and covered with an external skin. In the forward area, the duct wall is covered with aluminum machined skin. The intermediate and aft duct walls are covered with fiberglass honeycomb sandwich. The inboard wall of the duct is made up of a fixed duct and movable ramps which provide for a variable-geometry system for air induction control. The center beam consists of four main longerons, interconnecting shear panels, appropriate frames, and the forward nacelle attach point, and is the primary vertical bending member of the nacelle.

The engine compartment consists of the principal firewall bulkhead, the structure between the two engines, the primary engine attach points, and the aft nacelle attach points. Large hinged engine access doors are provided to complete the engine enclosure. Construction is frame, skin, and longeron.

The nacelle is attached to the aircraft at four points. The forward attach point is a single fitting on the top of the centerbeam structure, which is connected to the wing pivot pin through a ball joint. The other three

attach points are in the engine section in line with the rear engine support. They consist of links, two vertical and one horizontal, which connect the nacelle to the heavy support frame extending from the aft intermediate fuselage.

Horizontal Stabilizer

The horizontal stabilizer (figure A-5) consists of left and right slab panels attached to a steel spindle projecting out of the aft fuselage stub structure. Both left and right panels rotate on bearings and are independently controlled in order for the stabilizer to provide pitch and roll control of the aircraft. Each panel consists of a main structural box, a leading edge assembly, a trailing edge assembly, a tip assembly, an aerodynamics chord plane seal at the inboard end, and an air seal around the spindle.

Vertical Stabilizer

The vertical stabilizer consists of the main box structure, leading edge assembly, tip assembly, and trailing edge structure (figure A-6). The main box assembly supports the two upper rudder segments. Routing tunnels are provided in enclosed areas of the main box structure for electrical and cooling lines required to support avionics and antenna equipment in the tip and leading edge components. The rudder consists of three segments. The upper two segments are attached to the vertical stabilizer through power hinge fittings and actuated by hydraulic motors in the horizontal stabilizer actuator fairing. The lower rudder segment is supported by conventional hinge fittings and actuated by linear actuators between the rudder and aft fuselage structure.

The vertical stabilizer is attached to the aft fuselage principally through a double-shear attachment provided on the horizontal stabilizer spindle fitting. The vertical stabilizer is mechanically attached to the spindle fitting by close-tolerance, high-strength bolts.

NASTRAN MODEL PLANS

Detailed plans for the finite-element modeling of the A/C-2 structure, intended for use with the NASA/COSMIC release of NASTRAN level 16.0 on the DFRC CDC Cyber computer were prepared.

The detailed plans constrained the model to the minimum complexity to give satisfactory flexibility characteristics for FLEXSTAB aeroelastic analysis.

Included in the model plans are the control surfaces and provisions for their control system stiffnesses, as well as the secondary leading edge and trailing edge structure. The NASTRAN model plans specify seven substructures consisting of the following:

(1) Wing outer planel, flaps, slats, and outboard transition lugs

(2) Forward fuselage structure

(3) Aft fuselage structure, wing carry-through structure (WCTS), and inboard transition lugs

(4) Horizontal stabilizer, leading edge, and trailing edge

(5) Vertical stabilizer, leading edge, and rudders

(6) Overwing and underwing fairings

(7) Nacelle structure

In addition to modeling the B-1 A/C-2 airframe structure to represent the flexibility characteristics, the model was constructed to provide stress data at the airload survey strain gage locations for each component. In these regions, the model complexity was increased to provide the desired accuracy. In some regions, the complexity was dictated by the NASTRAN aspect ratio constraints. However, after considering all of these requirements and with considerable engineering restraint, the goal of utilizing less than 3600 grid points appears to be achievable.

The principal elements selected for use in the model are rods, bars, shear panels, isoparametric membranes, and plates. The fuselage shell consists of rods and shear panels, with isoparametric membranes used in selected regions where high aspect ratio dictates their desirability. The fuselage frames and bulkheads will utilize bars, rods, and shear panels. The wing and empennage structural model will consist of bending plates, bars, rods, shear panels, and membranes. The use of these elements and their distribution are shown in table I.

The model plans are described in the scaled model layouts showing the nodal point locations for each vehicle component and typical structural sizings for each component.

Detailed plans for the wing lower and upper surfaces are presented in figures B-1 and B-2. Wing detail views are shown in figure B-3.

TABLE I.- PRELIMINARY STATISTICS FOR ARS NASTRAN MODEL

Substructure No.	Description of component	NASTRAN model elements					
		No. of grids	Rod	Shear panel	Membrane	Plate	Bar
1	Wing, flaps, outboard lug	1000	550	275	775	175	400
2	Fwd fuselage	350	450	350	150	50	300
3	Aft fuselage, WCTS, inboard lug	650	600	700	250	275	550
4	Horizontal stabilizer	540	775	400	450	50	10
5	Vertical stabilizer	340	325	200	200	50	10
6	Fairings	300	150	50	30	200	100
7	Nacelle	340	650	150	50	250	500
	Total	3520	3500	2125	1905	1050	1870

Element		NASTRAN nomenclature
Rod	=	CONROD
Shear panel	=	CSHEAR
Membrane	=	CQDMEM 1
Plate	=	CQUAD 1 and CQUAD 2
Bar	=	CBAR

Plans for the forward fuselage substructure depicting the side, top, and bottom views are presented in figures B-4, B-5, and B-6. Details of the forward fuselage model are shown in figure B-7.

Aft fuselage model substructure plans depicting the side, top, and bottom views are presented in figure B-8, B-9, and B-10. Aft fuselage model details are shown in figure B-11.

Horizontal stabilizer model substructure plans are shown in figure B-12. Detail views of the horizontal stabilizer model and actuation system are presented in figure B-13.

Vertical stabilizer model substructure plans, including the leading edge, bullet fairing, and three rudders, are presented in figure B-14.

Plans for modeling the overwing and underwing fairing structures are presented in figure B-15. This complex structure includes the lower pivot fairing, upper pivot fairing, overwing movable fairing, forward intermediate fixed fairing, and underwing intermediate and aft fairing panels.

Plans for modeling the nacelle structure, including the engine access doors, are depicted in the views of the top nacelle, bottom nacelle, inboard nacelle, outboard nacelle, nacelle centerbody, and typical nacelle frames shown in figures B-16, B-17, B-18, B-19, B-20, and B-21, respectively.

ANALYSIS STRATEGY

General Problem Flow

NASTRAN, as described in ref. (1), consists of a number of subprograms or modules that are executed according to a sequence of macroinstructions controlled by the executive system. A number of such sequences, called rigid formats, are permanently stored in the program and can be selected by means of control cards. Each rigid format corresponds to a particular type of structural analysis. The user may, in addition, devise his own sequence of module calls, referred to as direct matrix abstract program (DMAP), for problems that do not conform to the one of the available rigid formats.

Figure 3 shows a simplified flow diagram for basic static analysis. Each block in the flow diagram represents a number of program modules. The structural matrix assembler generates stiffness and mass matrices for the grid point data obtained from tabular information generated by the input file processor and the geometry processor. The mass matrix is used in static

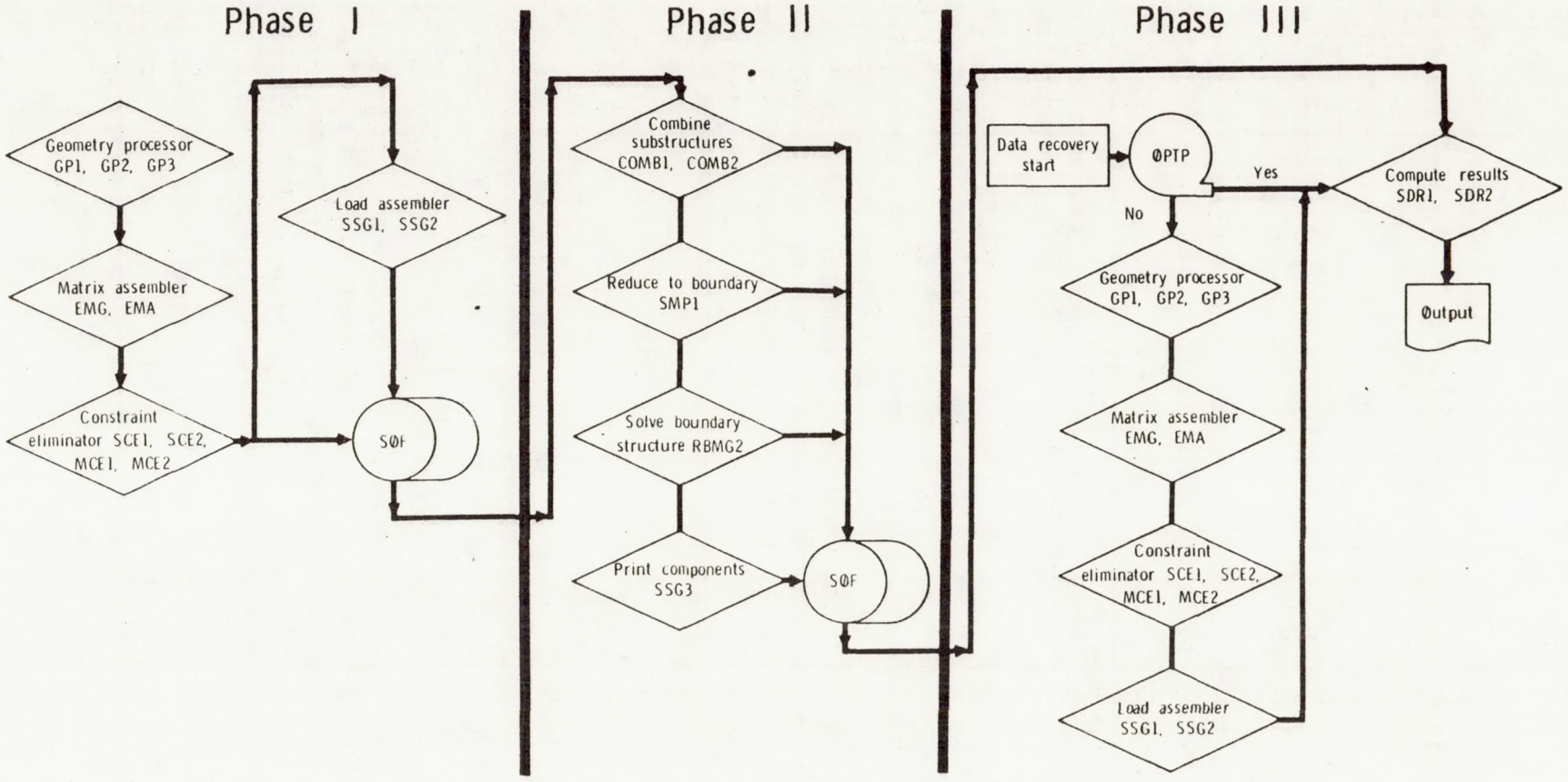

GP1, GP2, etc, are NASTRAN functional module names.

Figure 3.- NASTRAN flow chart.

analysis for the generation of gravity loads and inertia loads on unsupported structures. The stiffness matrix is reduced to the form in which it is finally solved through the imposition of single-point and multipoint constraints, and through the use of matrix partitioning. Load vectors are then generated from concentrated loads at grid points, pressure loads on surfaces, gravity, temperature, and enforced deformation, as appropriate, and are reduced to final form by the application of constraints and matrix partitioning. The solution for independent displacements is accomplished in two steps: (1) decomposition of the stiffness matrix [K] into upper and lower triangular factors, and (2) solution for (u) for specific load vectors (P), by means of successive substitution into the equations represented by the triangular factors of [K]. Dependent displacements are determined from the independent displacements by means of the equations of constraint.

Notation System

Many of the operations performed in computerized structural analysis are conveniently expressed in the notation of matrix algebra. In NASTRAN, as described in ref. 2, matrix arrays are represented by a root symbol that indicates the type of physical quantity and by one or more subscripts and superscripts that act as modifiers. The root symbols used in static analysis by the displacement method are listed in table II. Nearly all of the matrix

TABLE II. - ROOT SYMBOLS USED IN NASTRAN

$\{u\}$	Vector of displacement components
$\{P\}$	Vector of applied load components
$\{q\}$	Vector of forces of reaction
$\{Y\}$	Vector of enforced displacements
$[K]$	Stiffness matrix
$[M]$	Mass Matrix
$[B]$	Damping matrix
$[R]$	Matrix of constraint coefficients, as in $[R]\{u\} = 0$
$[G]$	Transformation matrix, as in $\{u_m\} = [G_m]\{u_n\}$

operations in static analysis are concerned with partitioning, merging, and transforming matrix arrays from one subset of displacement components to another. All components of displacement of a given type, such as all points constrained by single-point constraints, form a vector set that is distinguished by a subscript from other sets. A given component of displacement can belong to several vector sets. The mutually exclusive vector sets (u_p), the sum of whose members is the set of all physical components of displacement, are listed in table III.

TABLE III. - VECTOR SETS

u_m	Coordinates eliminated as independent degrees of freedom by multiglobal constraints
u_s	Coordinates eliminated by single-point constraints
u_o	Coordinates omitted by structural matrix partitioning (i.e., interior coordinates)
u_r	Coordinates to which determinate reactions are applied in static analysis
u_l	The remaining structural coordinates used in static analysis (points left over)
u_e	Extra degrees of freedom introduced in dynamic analysis to describe control systems, etc
u_a	$u_r + u_l$, the set left as analysis set for phase II
u_f	$u_a + u_o$, unconstrained free structural coordinates
u_n	$u_f + u_s$, all structural coordinates not constrained by multipoint constraints
u_g	$u_n + u_m$, all structural grid points including scalar points
u_p	$u_s + u_e$, all physical points

In static analysis (without substructuring), we are concerned only with the grid point set (u_g) and its subsets. The application of constraints and partitioning to the stiffness matrix involves the elimination of u_m, u_s, u_o, and u_r from u_g to form a stiffness matrix referred to u_l. For substructuring, it is necessary to perform matrix reduction as shown in phase II of figure 3.

Assembly of Structural Matrices

The element matrix generator (EMG) and the element matrix assembler (EMA) generate the stiffness, mass, and damping matrices for the structural model. For efficiency in restart, particularly when changing from statics to dynamics problems, the structural matrices, $[K_{gg}]$, $[K^4_{gg}]$, $[M_{gg}]$, and $[B_{gg}]$, are assembled by four separate executions of EMA. EMG generates the various types of structural matrices on a selective basis. A third part of the matrix assembly matrix operation (SMA3) adds the contributions of the general elements to the stiffness matrix.

The EMG refers to the appropriate "element" routines for calculation of the stiffness, mass, and damping matrices for each element. The matrices for each element are initially generated in an element coordinate system that is characteristic for each element type. The element matrices are transformed to the global coordinate system prior to transfer to direct access secondary storage.

The EMA assembles several columns of the structural matrices at one time. The number of columns assembled in one operation is limited by the space available in main storage. The required element matrices are transferred from secondary storage using the direct-access read operation. The completed columns of the structural matrices are written on secondary storage by using the regular NASTRAN pack routines.

Although the matrices generated by the structural matrix assembler are symmetric, complete columns are generated and retained for efficiency in succeeding matrix operations. This is necessary because all matrix operations are performed one column at a time and, in dynamics applications, the matrices are not necessarily symmetric. Moreover, the availability of symmetric matrices by rows or by columns is advantageous in some of the matrix operations.

Constraints and Partitioning

Structural matrices are initially assembled in terms of the set, u_g, of all structural grid points, excluding only the set, u_e, of extra points used in dynamic analysis. The following paragraphs describe the subsequent

reduction of the structural matrices to the set, u_1, which is the set of coordinates that remains after all constraint and partitioning operations have been performed, and which is, therefore, the first set to be evaluated in static analysis.

The structural matrices whose assembly is discussed in the preceeding paragraphs are:

(1) $[K_{gg}]$ the structural stiffness matrix due to elastic structural elements

(2) $[K^4_{gg}]$ the structural damping matrix of imaginary stiffness coefficients

(3) $[B_{gg}]$ the viscous damping matrix due to damper elements

(4) $[M_{gg}]$ the structural mass matrix

The reduction procedures for the $[K_{gg}]$ matrix are explained in the following paragraphs.

Multipoint Constraints

The multipoint constraint equations are initially expressed in the form,

$$[R_g]\ (u_g) = 0, \tag{1}$$

where the coefficients are supplied by the user. The user also specifies the degree of freedom that is made dependent by each equation of constraint, so that the (u_g) matrix may immediately be partitioned into two subsets,

$$(u_g) = \left\{ \frac{u_n}{u_m} \right\}, \tag{2}$$

where the set, u_m, is the set of dependent degrees of freedom. The matrix of constraint coefficients is similarly partitioned

$$[R_g] = [R_n \mid R_m], \tag{3}$$

so that equation 1 becomes

$$[R_n]\ (u_n) + [R_m]\ (u_m) = 0 \tag{4}$$

$[R_m]$ is a nonsingular matrix. We can, therefore, form the multipoint constraint matrix,

$$[G_m] = - [R_m]^{-1} [R_n], \tag{5}$$

so that equation 4 may be stated as

$$(u_m) = [G_m] (u_n). \tag{6}$$

Prior to the imposition of constraints, the structural problem may be written as

$$[K_{gg}] (u_g) = (P_g), \tag{7}$$

or, partitioning in terms of the coordinate sets, u_n and u_m

$$\left[\begin{array}{c|c} \bar{K}_{nn} & K_{nm} \\ \hline K_{nm}^T & K_{mm} \end{array}\right] \left\{\begin{array}{c} u_n \\ \hline u_m \end{array}\right\} = \left\{\begin{array}{c} \bar{P}_n \\ \hline P_m \end{array}\right\} \tag{8}$$

Bars over symbols are used to designate arrays that are replaced in the reduction process.

The addition of constraints to the structure requires that the forces of constraint be added to the equilibrium equations. The forces of constraint are proportional to the corresponding coefficients in the constraint equations. Thus, writing the equilibrium and constraint equations together in partitioned form,

$$\left[\begin{array}{c|c|c} \bar{K}_{nn} & K_{nm} & G_m^T \\ \hline K_{nm}^T & K_{mm} & -I \\ \hline G_m & -I & 0 \end{array}\right] \left\{\begin{array}{c} u_n \\ \hline u_m \\ \hline q_m \end{array}\right\} = \left\{\begin{array}{c} \bar{P}_n \\ \hline P_m \\ \hline 0 \end{array}\right\} \tag{9}$$

where $[q_m]$ is the vector of constraint forces (u_m). Straightforward elimination of u_m and q_m gives

$$\left[\bar{K}_{nn} + K_{nm} G_m + G_m^T K_{nm}^T + G_m^T K_{mm} G_m\right] (u_n) = (\bar{P}_n) + \left[G_m^T\right] (P_m), \tag{10}$$

or

$$[K_{nn}]\ (u_n) = (P_n), \tag{11}$$

where

$$K_{nn} = \overline{K}_{nn} + K_{nm}G_m + G_m^T K_{nm}^T + G_m^T K_{mm} G_m, \tag{12}$$

and

$$P_n = \overline{P}_n + G_m^T P_m. \tag{13}$$

The initial partition of K_{gg} and the operations indicated by equations 5, 12, and 13 are performed by appropriate modules of the program. The multipoint matrix, G_m, is used in structural matrix reduction (equation 12), load vector reduction (equation 13), and data recovery (equation 6). It is saved for these purposes in an auxiliary storage file. The other structural matrices, $[K_{gg}^4]$, $[B_{gg}]$ and $[M_{gg}]$, are transformed by formulas that are identical in form to equation 12.

Single-Point Constraints

Single-point constraints are applied to the set, u_s, in the form

$$(u_s) = (Y_s), \tag{14}$$

where (Y_s) is a vector of enforced deformations, any or all of whose elements may be zero. The set, u_n, is partitioned into u_s and u_f (the free or unconstrained set)

$$(u_n) = \begin{Bmatrix} u_f \\ \hline u_s \end{Bmatrix}. \tag{15}$$

The stiffness matrix, K_{nn}, is similarly partitioned

$$[K_{nn}] = \left[\begin{array}{c|c} K_{ff} & K_{fs} \\ \hline K_{fs}^T & K_{ss} \end{array}\right] \tag{16}$$

The complete structural equations, including the single-point forces of constraint, q_s, may be written in partitioned matrix form as

$$\left[\begin{array}{c|c|c} K_{ff} & K_{fs} & 0 \\ \hline K_{fs}^T & K_{ss} & -I \\ \hline 0 & I & 0 \end{array}\right] \left\{\begin{array}{c} u_f \\ \hline u_s \\ \hline q_s \end{array}\right\} = \left\{\begin{array}{c} \bar{P}_f \\ \hline P_s \\ \hline Y_s \end{array}\right\} \tag{17}$$

Straightforward elimination gives

$$[K_{ff}]\ (u_f) = (\bar{P}_f) - [K_{fs}]\ (Y_s) = (P_f). \tag{18}$$

The forces of constraint are recovered by means of the middle row of equation 17; i.e.,

$$(q_s) = -\ (P_s) + [K_{fs}^T]\ (u_f) + [K_{ss}]\ (u_s). \tag{19}$$

Thus, all three of the distinct partitions of K_{nn} (i.e., K_{ff}, K_{fs} and K_{ss}) are needed in subsequent calculations and are placed in auxiliary storage. For the other structural matrices (K^4_{nn}, B_{nn}, and M_{nn}), only the (ff) partitions are saved. The assumption is made, implicitly, that the effects of the other structural matrices on the single-point forces of constraint may be ignored.

Partitioning

At user option, the set of free coordinates, u_f, may be partitioned into two sets, u_o and u_a, such that the u_o set is eliminated first. Thus,

$$(u_f) = \left\{\begin{array}{c} u_a \\ \hline u_o \end{array}\right\}. \tag{20}$$

The equilibrium equations after the elimination of constraints (equation 18) may be written in partitioned form as

$$\left[\begin{array}{c|c} \bar{K}_{aa} & K_{ao} \\ \hline K_{ao}^T & K_{oo} \end{array}\right] \left\{\begin{array}{c} u_a \\ \hline u_o \end{array}\right\} = \left\{\begin{array}{c} \bar{P}_a \\ \hline P_o \end{array}\right\}. \tag{21}$$

Rearrange the bottom half of equation 21

$$[K_{oo}]\ (u_o) = (P_o) - [K_{ao}]^T\ (u_a) \tag{22}$$

and solve for (u_o):

$$(u_o) = [K_{oo}]^{-1}\ (P_o) - [K_{oo}]^{-1}\ [K_{ao}]^T\ (u_a). \tag{23}$$

(Note that, in practice, stiffness matrices are never inverted due to excessive computer running time. The practical alternative will be explained presently.) Substitute for u_o into the top half of equation 21:

$$[\bar{K}_{aa} - K_{ao}K_{oo}^{-1}\ K_{ao}^T]\ (u_a) = (\bar{P}_a) - [K_{ao}]\ [K_{oo}]^{-1}\ (P_o). \tag{24}$$

It is convenient to define the matrix

$$[G_o] = -\ [K_{oo}]^{-1}\ [K_{ao}]^T, \tag{25}$$

so that equation 24 becomes

$$[\bar{K}_{aa} + K_{ao}G_o]\ (u_a) = (\bar{P}_a) + [G_o]^T\ (P_o), \tag{26}$$

where advantage is taken of the symmetry of $[K_{oo}]$.

Following the practice of condensation established in preceding paragraphs,

$$[K_{aa}]\ (u_a) = (P_a), \tag{27}$$

where

$$[K_{aa}] = [K_{aa}] + [K_{ao}]\ [G_o] \tag{28}$$

$$(P_a) = (\bar{P}_a) + [G_o]^T\ (P_o) \tag{29}$$

The $[G_o]$ matrix defined in equation 25 is obtained practically from the solution of

$$[K_{oo}]\ [G_o] = -\ [K_{ao}]^T, \tag{30}$$

where $[K_{ao}]^T$ is treated as a set of load vectors. Each such vector produces a column of $[G_o]$. The $[K_{oo}]$ matrix is first decomposed into lower and upper triangular factors. Once (u_a) is obtained, the set of omitted coordinates, (u_o), is obtained as follows. Define the set (u_o^o) as the solution of

$$[K_{oo}]\ (u_o^o) = (P_o) \tag{31}$$

Note that the triangular factors of $[K_{oo}]$ obtained in connection with equation 30 are saved for use in connection with equation 31, which cannot be solved until the load vector (P_o) is formed. Then, using equations 25 and 31 in equation 22,

$$(u_o) = (u_o^o) + [G_o]\ (u_a). \tag{32}$$

The Guyan Reduction

The Guyan Reduction (ref. 3) is a means for reducing the number of degrees of freedom used in dynamic analysis with minimum loss of accuracy. Its basis is that fewer grid points are needed to describe the inertia of a structure than are needed to describe its elasticity with comparable accuracy. If inertia properties are rationally redistributed to a smaller set of grid points, the remaining grid points can be assigned to the u_o set described in the preceding paragraphs and eliminated, leaving only the smaller u_a set for dynamic analysis.

In the Guyan Reduction, the means by which inertia and damping are redistributed are to consider the $[G_o]$ matrix of the preceding paragraphs as a set of rigid constraints, such that

$$(u_o) = [G_o]\ (u_a). \tag{33}$$

The $[G_o]$ matrix now has the same implications for the u_o coordinates that the multipoint constraint matrix, $[G_m]$, has for the u_m coordinates (equation 6). The reduced structural mass matrix is, by analogy with equation 12,

$$[M_{aa}] = [\bar{M}_{aa} + M_{ao}\ G_o + G_o^T\ M_{ao}^T + G_o^T\ M_{oo}\ G_o]. \tag{34}$$

The reduced damping matrices, $[K^4_{aa}]$ and $[B_{aa}]$, are formed in the same manner. The structural stiffness matrix $[K_{aa}]$, is given by equation 28. The reduced dynamic load vactor is, by analogy with equation 13.

$$(P_a) = (\bar{P}_a + G_o^T P_o). \tag{35}$$

The approximation made in the Guyan Reduction is that the (u_o^o) in equation 32 is neglected; i.e., that the deformations of the u_o set relative to the u_a set due to inertial and other loads applied to the u_o set are neglected. The error in the approximation is small, provided that the (u_a) set is judiciously chosen. The selection should be based, in part, on an estimate of the relative deformation, (u_o^o). Thus, the members of u_a should be uniformly dispersed throughout the structure and should include all large mass items. The basic assumption made in the Guyan Reduction is identical to that made in forming consistent mass matrices for individual elements.

DMAP PROGRAMMING PLANS FOR FLEXSTAB

Detail plans for DMAP programming of the NASTRAN model to produce the input data required for FLEXSTAB Level 1.02.00 will be accomplished during the structural component model generation. The development of these plans includes the selection of the grid points to be retained for use in the FLEXSTAB model. It is planned that the initial selection of points will be reviewed by NASA DFRC and AFFDL technical personnel for conformation. These final selected points will then be utilized using the OMIT and/or ASET cards to achieve the matrix reduction, with the suitable matrix being generated within the NASTRAN computer program processing. The desired flexibility matrix can be generated for use by FLEXSTAB by using the OUTPUT2 module in conjunction with the SOLVE module of NASTRAN. Since there has been limited application of NASTRAN Level 16.0 in conjunction with FLEXSTAB Level 1.02.00, the technical personnel from Rockwell, NASA DFRC, and AFFDL will jointly develop the detailed plan for the DMAP programming.

Appendix A

FIGURES USING ENGINEERING UNITS

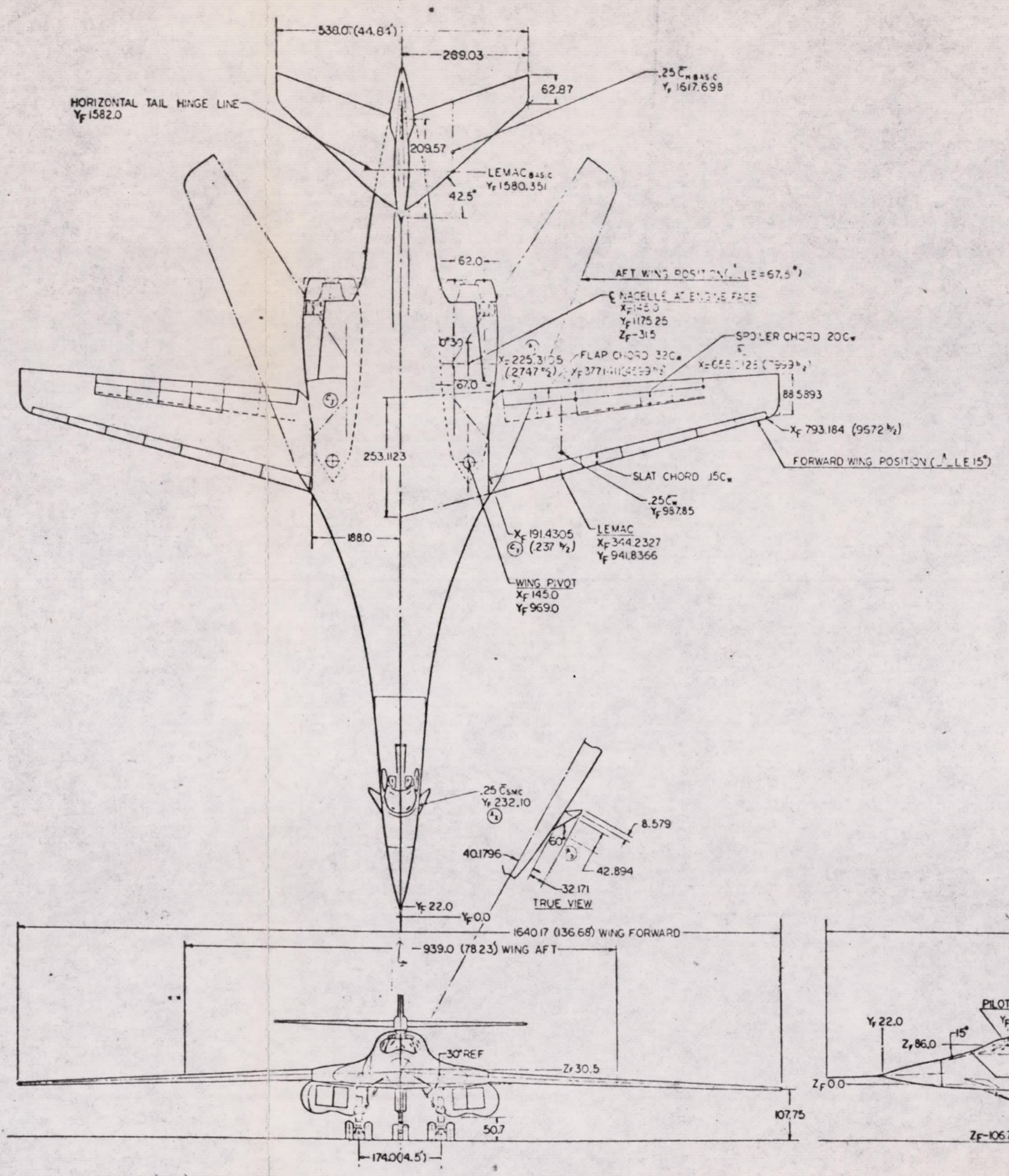

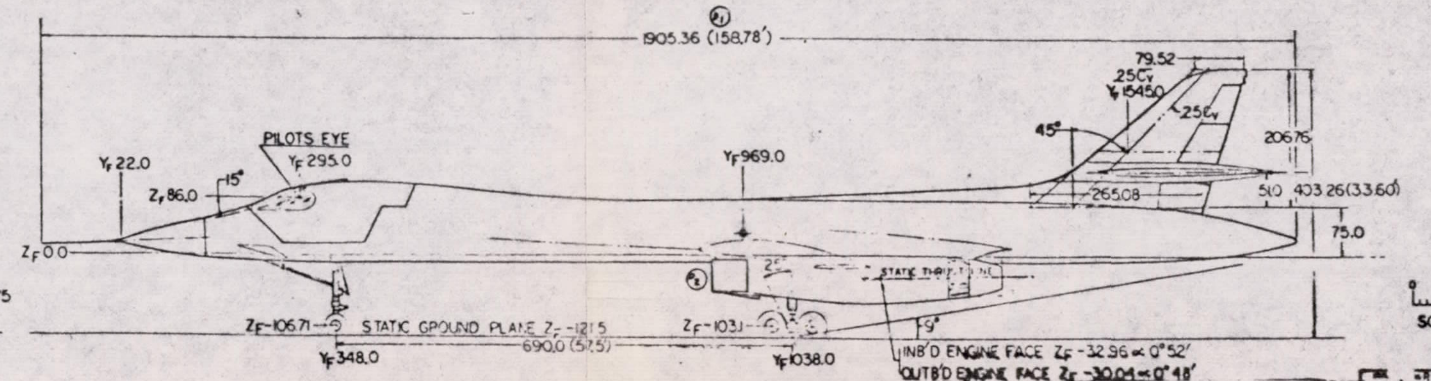

GEOMETRIC DATA

ITEM	WING FWD POSITION	WING AFT POSITION	HORIZONTAL TAIL TOTAL	VERTICAL TAIL TOTAL	STRUCTURAL MODE CONTROL
AREA ~ SQ. FT.	1946.0	1946 (REF)	509.0	247.4	11.5
ASPECT RATIO	9.6	3.14	3.95	1.2	2.5
TAPER RATIO	.35	—	.30	.30	.20
THICKNESS RATIO	REF: LINES DRAWING NA69-1902 DB-2.14		REF: MDID 2.14	.10 ROOT .05 Z_F 126.0 TO TIP	.05
AIRFOIL SECTION				65A010 ROOT 65A005 Z_F 26.0 TO TIP	65A005
LEADING EDGE SWEEP	15.0°	67.5°	42.5°	45° AT .25C	60°
DIHEDRAL ANGLE	-1.94°	—	0°	—	-30.0°
INCIDENCE ANGLE	2° ANF 65.6° 0° TIP	—	0°	—	DEFL ± 20.0°
MAC LENGTH - INCHES	154.053	—	149.385	188.954	29.55
M.A.C. LOCATION - INCHES	344.2327	—	110.373	84.825	12.510 TRUE

CONTROL SURFACE DATA

ITEM	FLAP	SPOILER	SLAT	RUDDER	HORIZ. TAIL
TYPE	SINGLE-SLOTTED	UPPER SURFACE ONLY	POWERED	—	ALL MOVABLE
AREA - SQ FEET	310.38	115.0	187.62	60.6	474.5
DEFLECTION	25°	0° TO 70° UP	20.0°	FLAP DN ±25° FLAP UP ±10°	PITCH +10° -25° ROLL ±20°

LANDING GEAR DATA

ITEM	MAIN	AUXILIARY
TIRE SIZE & TYPE	C44.5×16.0-21 TWIN TANDEM	35×11.5-16 TWIN
PLY RATING	24	24
ROLLING RADIUS - INCHES	18.4	14.79
FLAT RADIUS - INCHES	13.6	11.3
STRUT-TOTAL STROKE-IN	16.5	22.0
STRUT-STATIC TO COMPRESSED	3.5	7.0

PROPULSION DATA

FOUR 100% SIZE GENERAL ELECTRIC YF101 - GE - 100 ENGINES

2-D VARIABLE RAMP INLETS-CAPTURE AREA = 1441 SQ. IN. PER ENGINE

WEIGHT DATA

AIRCRAFT EMPTY WEIGHT	~ LB =	SEE SDM CODE II B-7
DESIGN USEFUL LOAD	~ LB =	SEE SDM CODE II B-7
DESIGN GROSS WEIGHT-TAXI	~ LB =	360,000
MAXIMUM GROSS WEIGHT	~ LB =	391,000

Preceding Page Blank

Figure A-1. - General arrangement - RDT&E A/C-1 and-2

B-1 GENERAL ARRANGEMENT

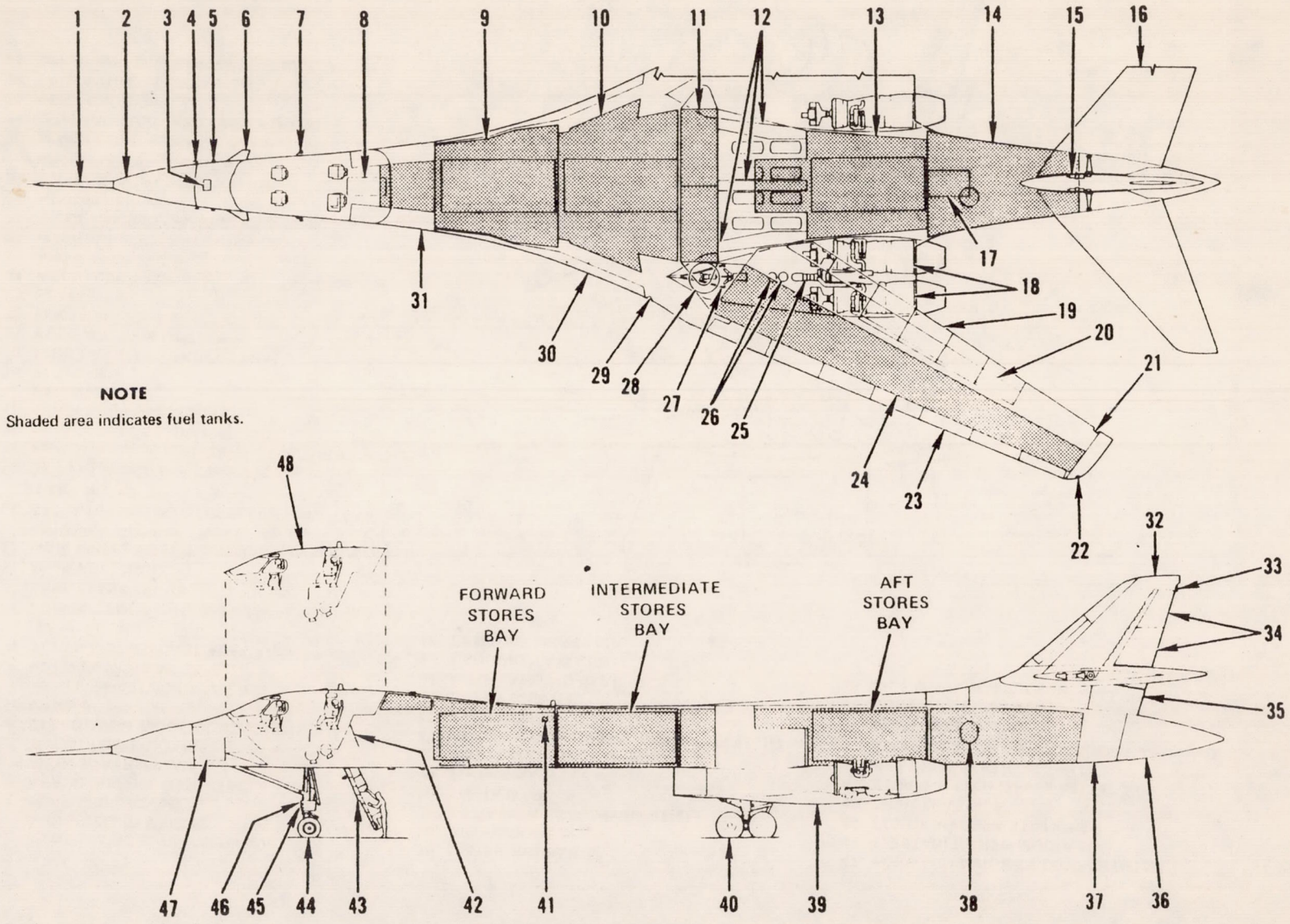

NOTE

Shaded area indicates fuel tanks.

Figure A-1. - Continued.

1. PITOT-STATIC BOOM (WITH AOA AND SIDESLIP VANES)
2. FORWARD RADOME
3. AERIAL REFUEL RECEPTACLE
4. PITOT-STATIC PROBE *
5. TOTAL TEMPERATURE PROBE *
6. STRUCTURAL MODE CONTROL SYSTEM VANE *
7. ANGLE-OF-ATTACK VANE *
8. CREW ENTRY WAY
9. FORWARD FUSELAGE FUEL TANK (TANK NO. 1)
10. FORWARD INTERMEDIATE FUSELAGE FUEL TANK (TANK NO. 2)
11. MAIN FUEL TANKS
12. MAIN WHEEL WELL EQUIPMENT (INTERMEDIATE AVIONICS) COMPARTMENT
13. AFT INTERMEDIATE FUSELAGE FUEL TANK (TANK NO. 3)
14. AFT FUSELAGE FUEL TANK (TANK NO. 4)
15. HORIZONTAL STABILIZER ACTUATOR *
16. HORIZONTAL STABILIZER
17. FLIGHT CONTROLS MIXER BAY
18. ENGINES *
19. FLAPS (6) *
20. SPOILERS/SPEED BRAKES (4) *
21. FUEL JETTISON OUTLET *
22. POSITION LIGHT *
23. SLATS (7) *
24. WING FUEL TANK *
25. APU *
26. HYDRAULIC RESERVOIRS *
27. INLET RAMP MECHANISM *
28. WING PIVOT
29. SUPPLEMENTAL POSITION AND ANTICOLLISION LIGHT *
30. WING GLOVE AVIONICS COMPARTMENT *
31. CENTRAL AVIONICS COMPARTMENT
32. VERTICAL STABILIZER
33. TAIL/ANTICOLLISION LIGHT
34. UPPER AND INTERMEDIATE RUDDERS
35. LOWER RUDDER
36. AFT RADOME
37. AFT AVIONICS COMPARTMENT
38. LN_2 DEWAR
39. ENGINE NACELLE *
40. MAIN LANDING GEAR *
41. AERIAL REFUEL/WING INSPECTION LIGHT *
42. ENTRY DOOR
43. ENTRY LADDER
44. NOSE LANDING GEAR
45. LANDING/TAXI LIGHT
46. LANDING LIGHTS (2)
47. FORWARD AVIONICS COMPARTMENT
48. EJECTABLE CREW MODULE
49. FORWARD CREW STATIONS
50. CREW SEAT (4) †
51. ESCAPE HATCH (SEVERABLE)
52. AFT CREW STATIONS
53. CONTROLS FOR ENTRY LADDER, APU, AND MAIN GEAR DOORS
54. SURVIVAL EQUIPMENT
55. SIDE WINDOW (SEVERABLE) *

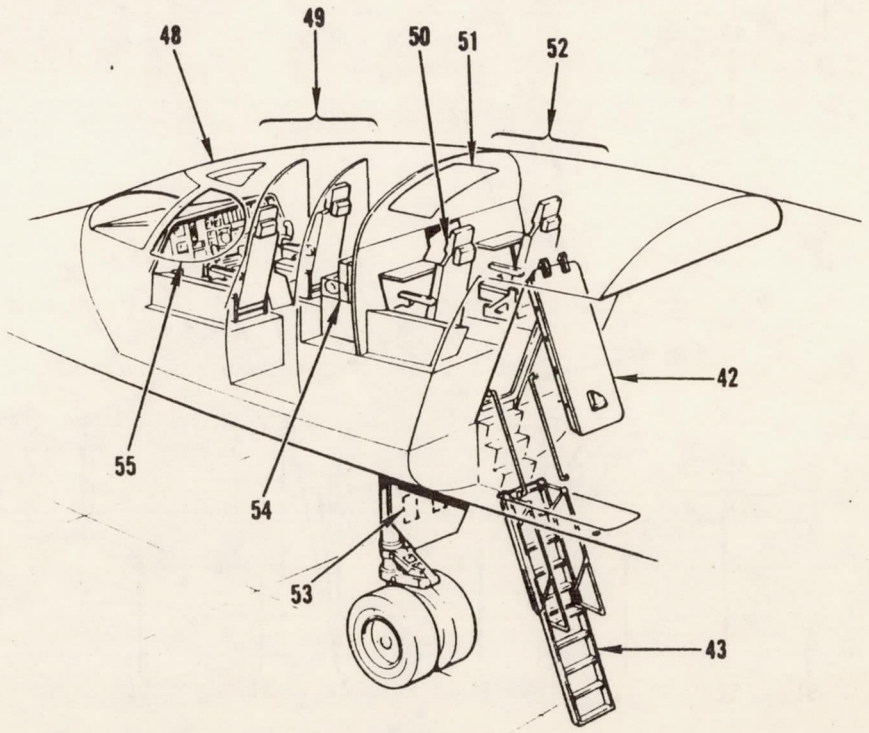

B 11048

* Both Sides (L and R)

† Right aft seat temporarily removed

Figure A-1. - Concluded.

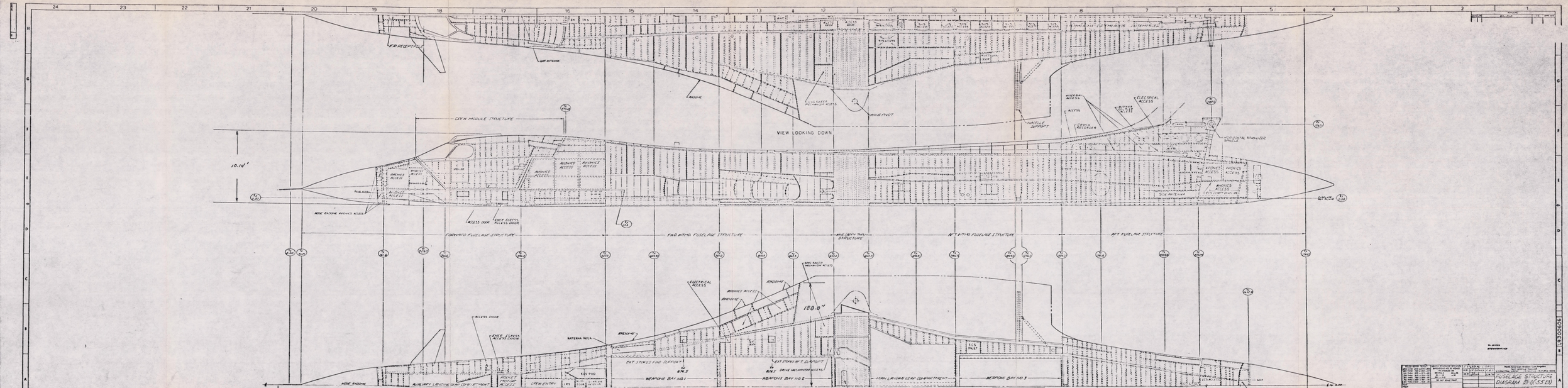

Figure A-2. - Fuselage structure diagram (B-1) (-55B).

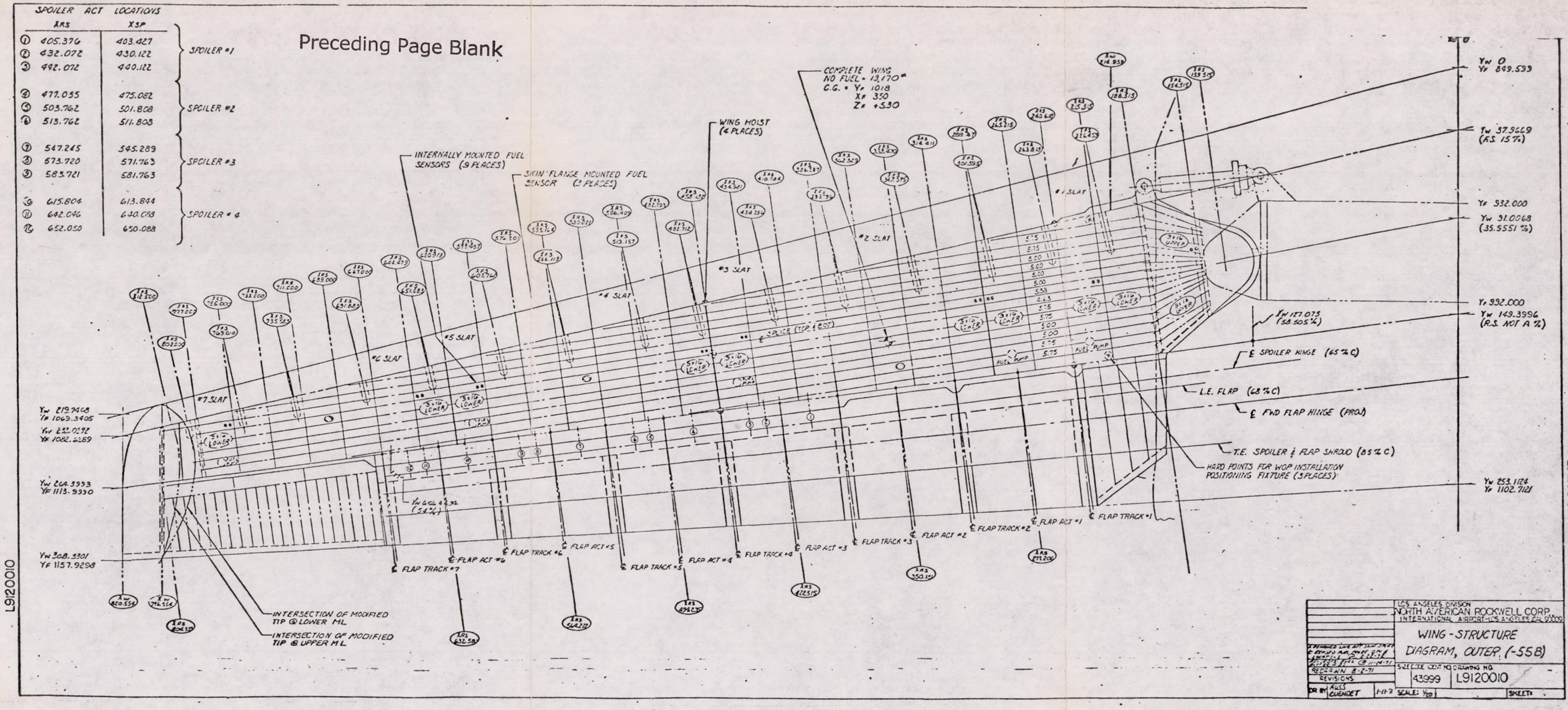

Figure A-3. - Wing-structure diagram, outer (-55B).

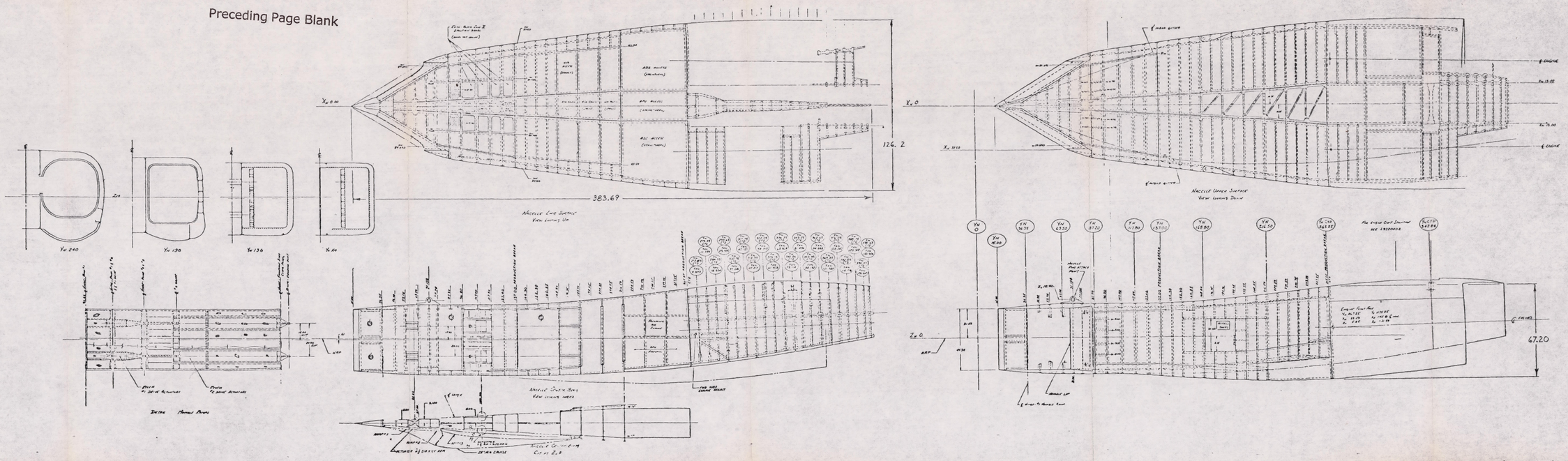

Figure A-4. - Structural arrangement - nacelle external compression inlet (RDTE).

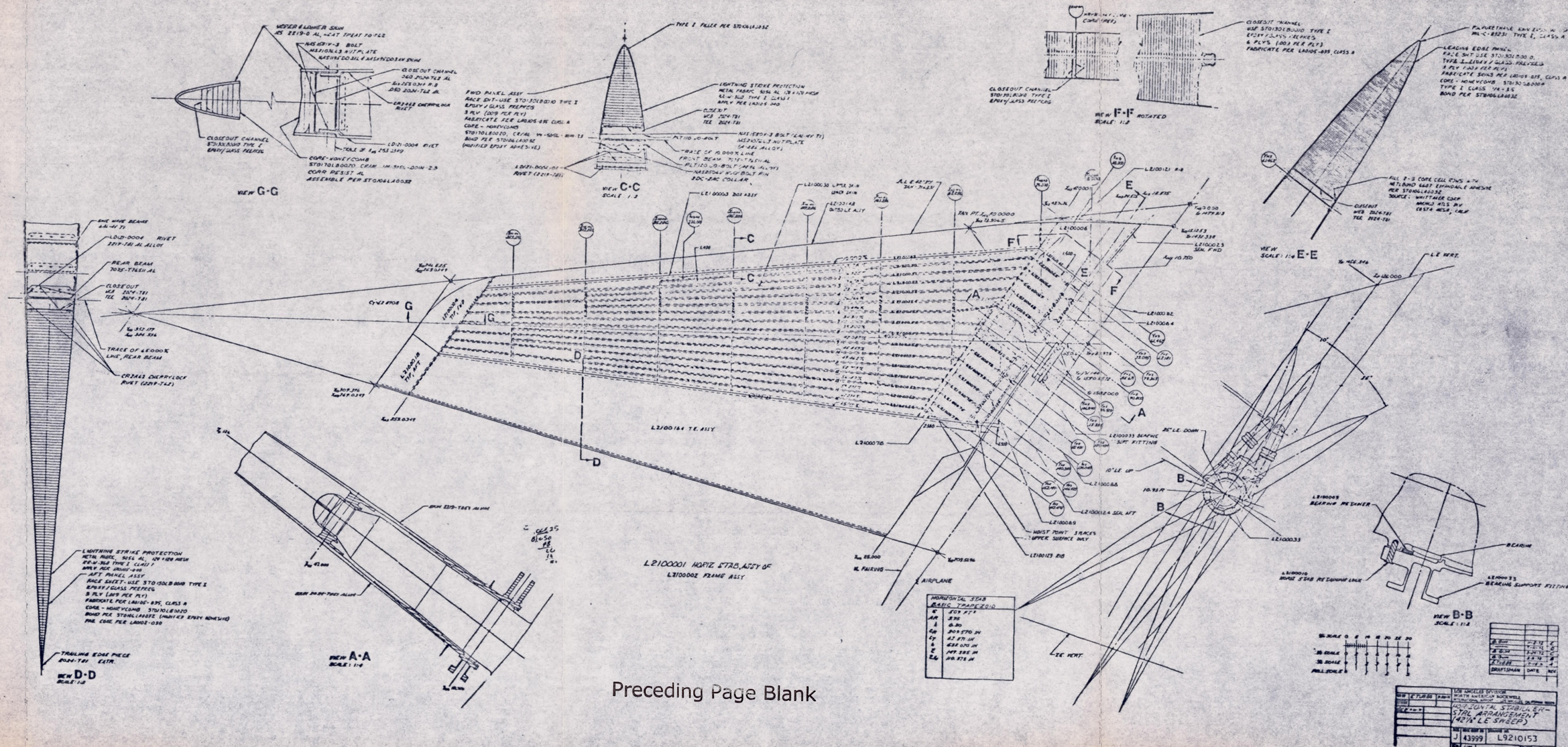

Preceding Page Blank

Figure A-5. - Horizontal stabilizer - STRL arrangement (42-1/2° LE sweep).

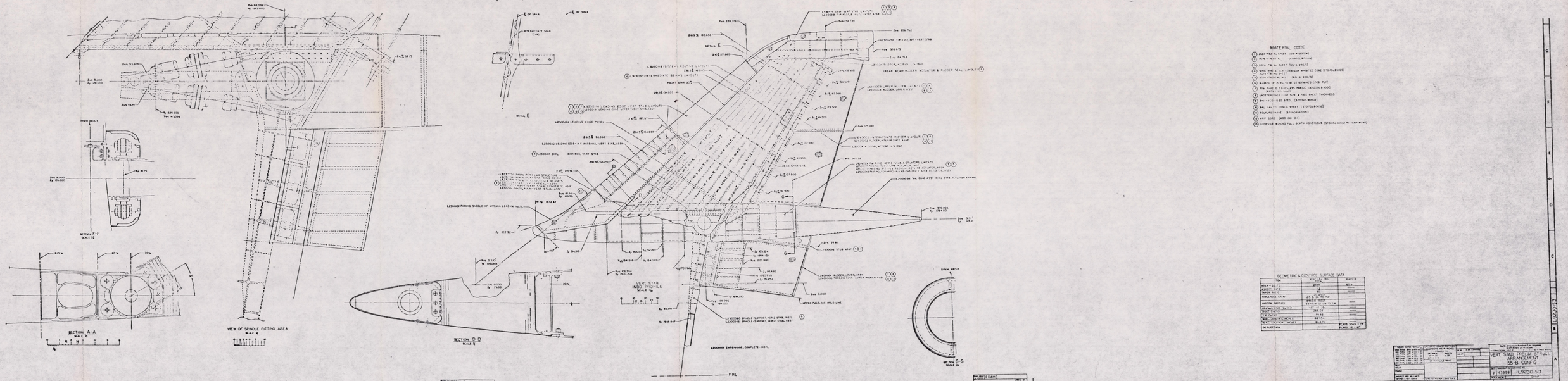

Figure A-6. - Vertical stabilizer structural arrangement.

Appendix B

NASTRAN MODEL SCALE DRAWINGS

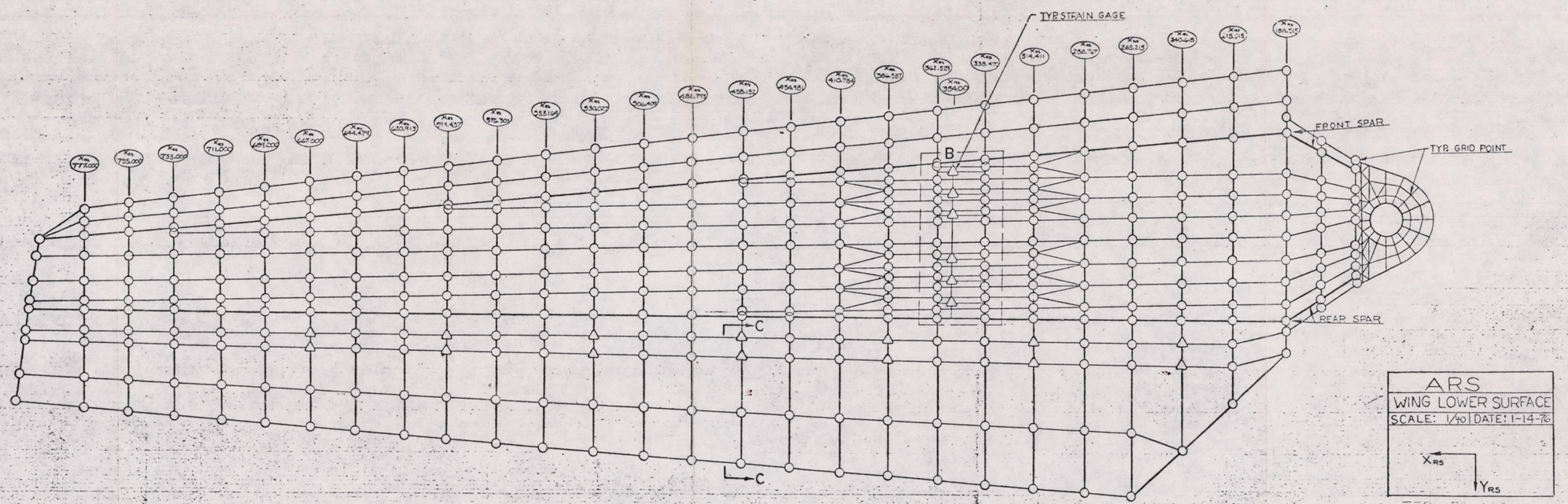

Figure B-1. - Wing lower surface.

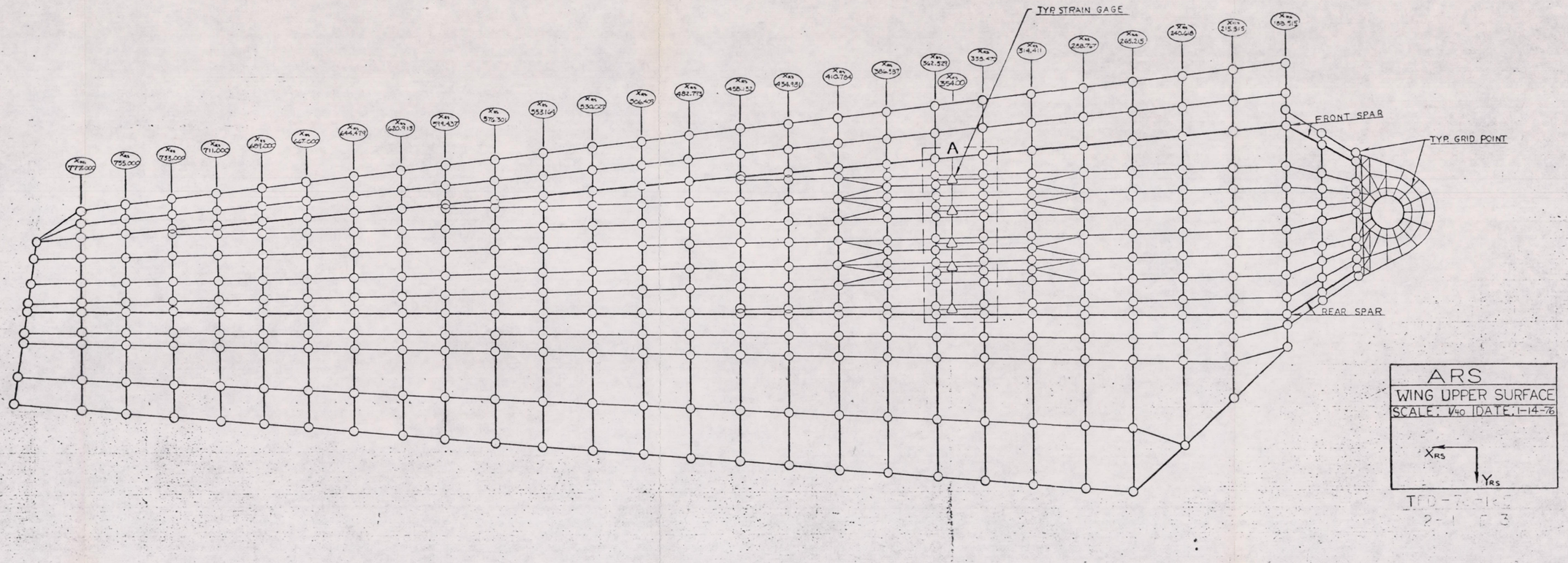

Figure B-2. - Wing upper surface.

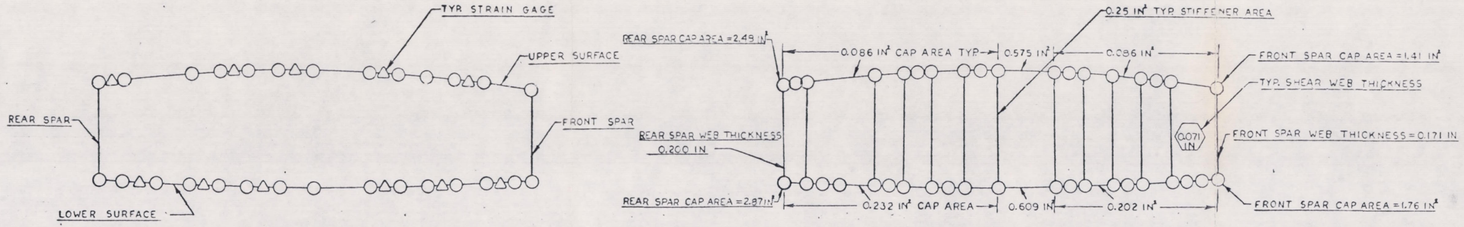

VIEW OF WING RIB
AT X_{RS} 354.00
SCALE: 1/6

VIEW OF WING RIB
AT X_{RS} 362.529
SCALE: 1/6

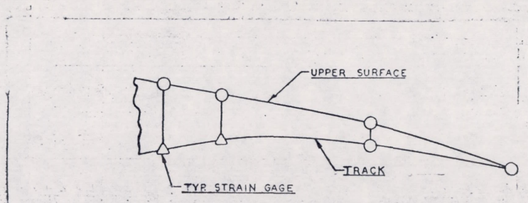

VIEW C-C
FLAP TRACK NO. 4
SCALE: 1/6

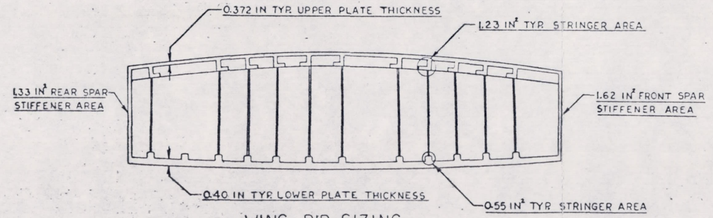

WING RIB SIZING
AT X_{RS} 362.529
SCALE: 1/6

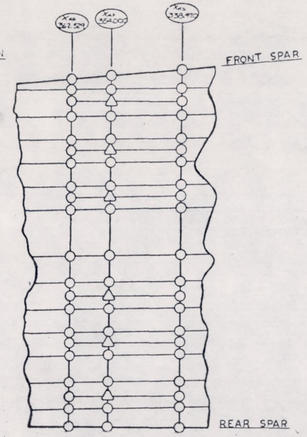

VIEW B
WING LOWER SURFACE
SCALE: 1/20

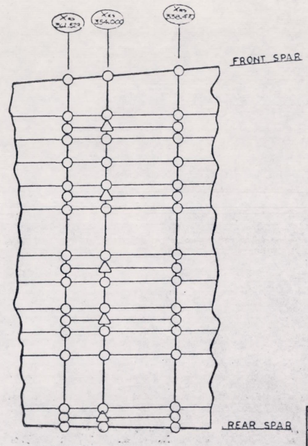

VIEW A
WING UPPER SURFACE
SCALE: 1/20

ARS
WING DETAIL VIEWS
SCALE: NOTED DATE: 1-14-76

Figure B-3. - Wing detail views.

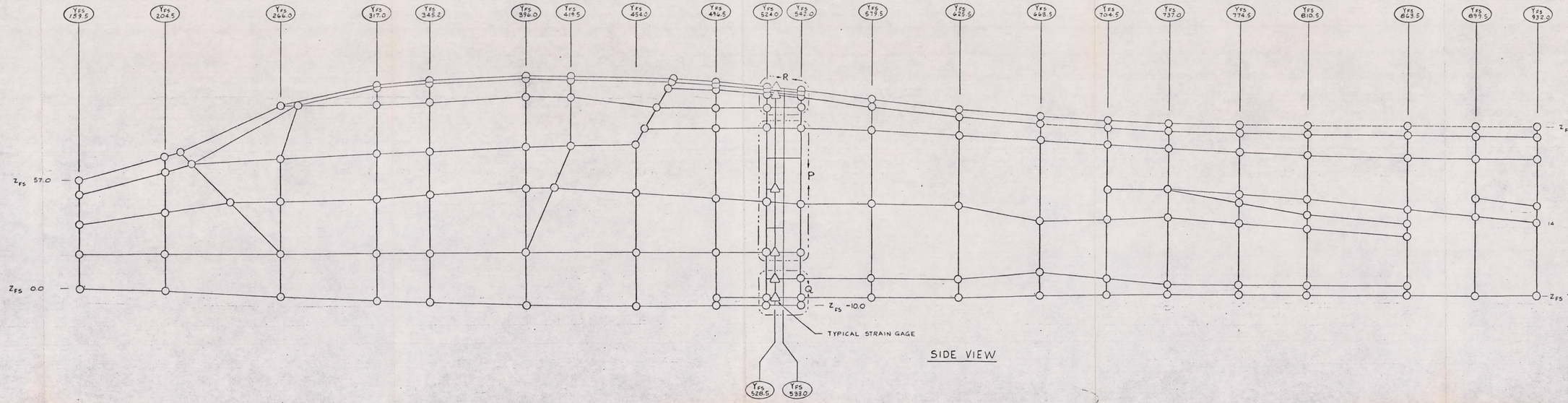

SIDE VIEW

AIRLOADS RESEARCH STUDY	
FWD. FUSELAGE SIDE VIEW	
SCALE: 1/20	DATE: 3 FEB 76
DWN BY: R. LATHAM	CHK BY: L. SHAH

Z_{FS}
Y_{FS}

Figure B-4. - Forward fuselage side view.

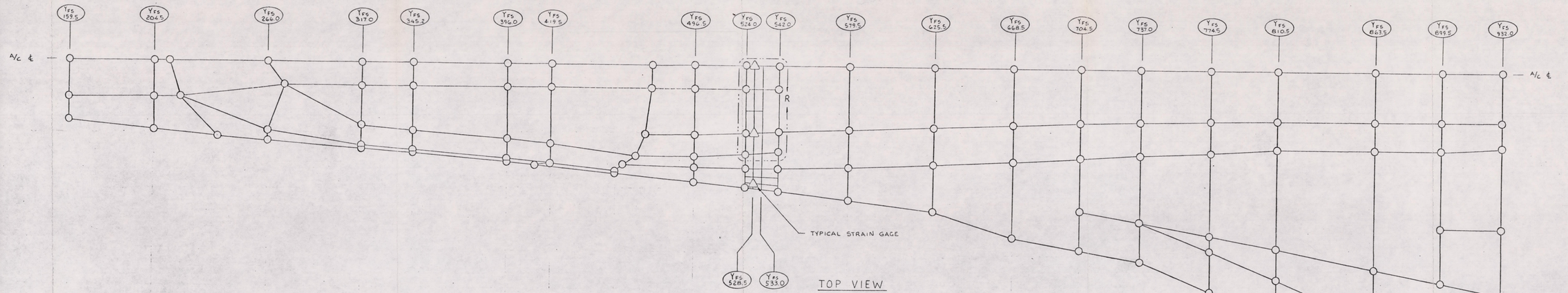

AIRLOADS RESEARCH STUDY	
FORWARD FUSELAGE TOP VIEW	
SCALE : 1/20	DATE 3 FEB. 76
DWN. BY : R. LATHAM	CHK BY : L. SHAH

Y_{FS}

X_{FS}

Figure B-5. - Forward fuselage top view.

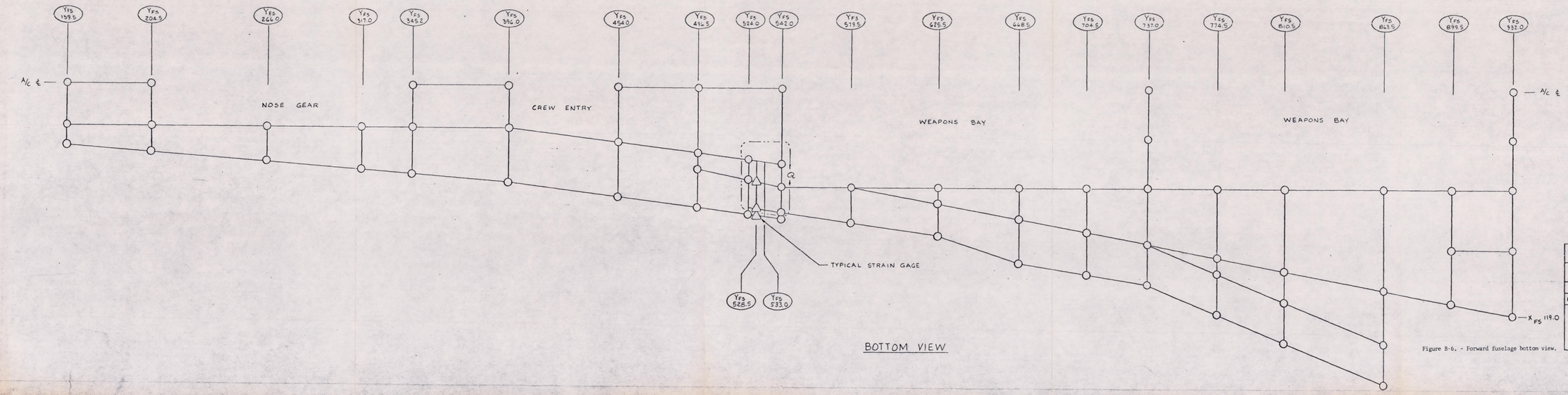

AIRLOADS RESEARCH STUDY	
FWD. FUSELAGE BOTTOM VIEW	
SCALE: 1/20	DATE: 3 FEB. 76
DWN BY: R. FISLER	CHK BY: R LATHAM

Figure B-6. - Forward fuselage bottom view.

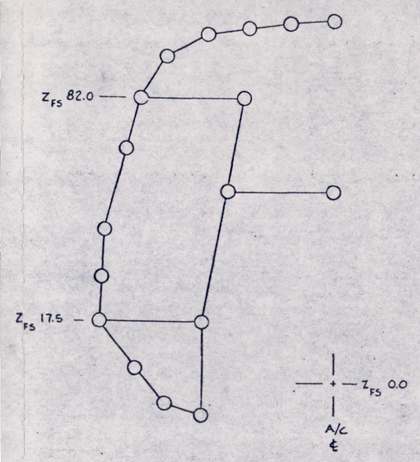

Y_{FS} 524.0

VIEW LOOKING FORWARD

SCALE: 1/20

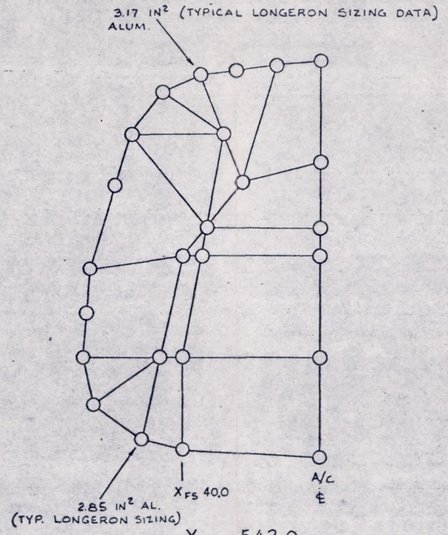

Y_{FS} 542.0

VIEW LOOKING FORWARD

SCALE: 1/20

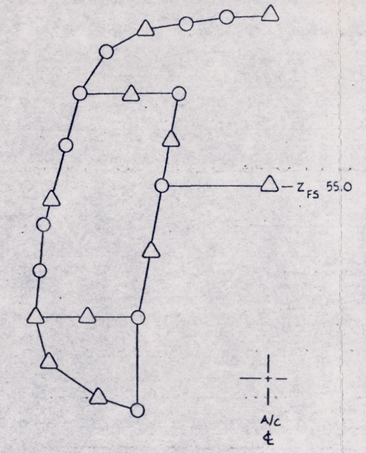

Y_{FS} 528.5

VIEW LOOKING FORWARD

SCALE: 1/20

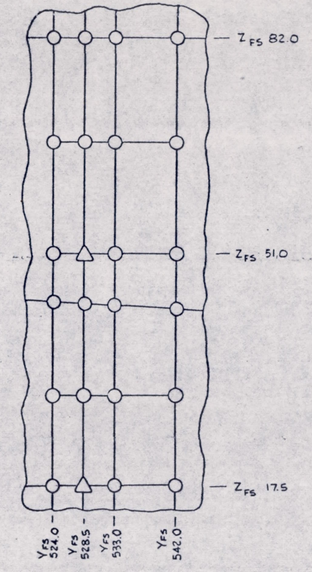

VIEW "P"

SIDE VIEW

SCALE: 1/10

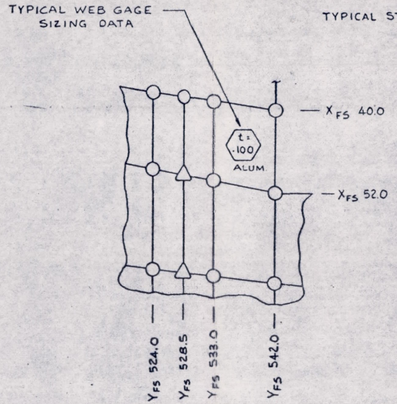

VIEW "Q"

BOTTOM VIEW

SCALE: 1/10

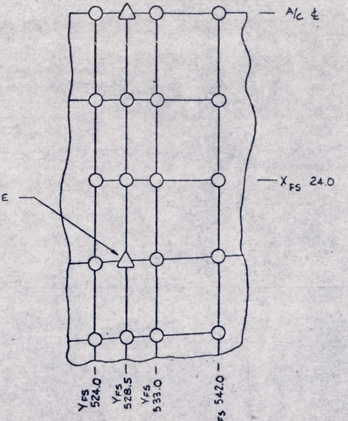

VIEW "R"

TOP VIEW

SCALE: 1/10

AIRLOADS RESEARCH STUDY	
FORWARD FUSELAGE DETAILS	
SCALE: NOTED	DATE: 3 FEB. 76
DWN. BY: R. LATHAM	CHK BY: L. SHAH

Figure B-7. - Forward fuselage details.

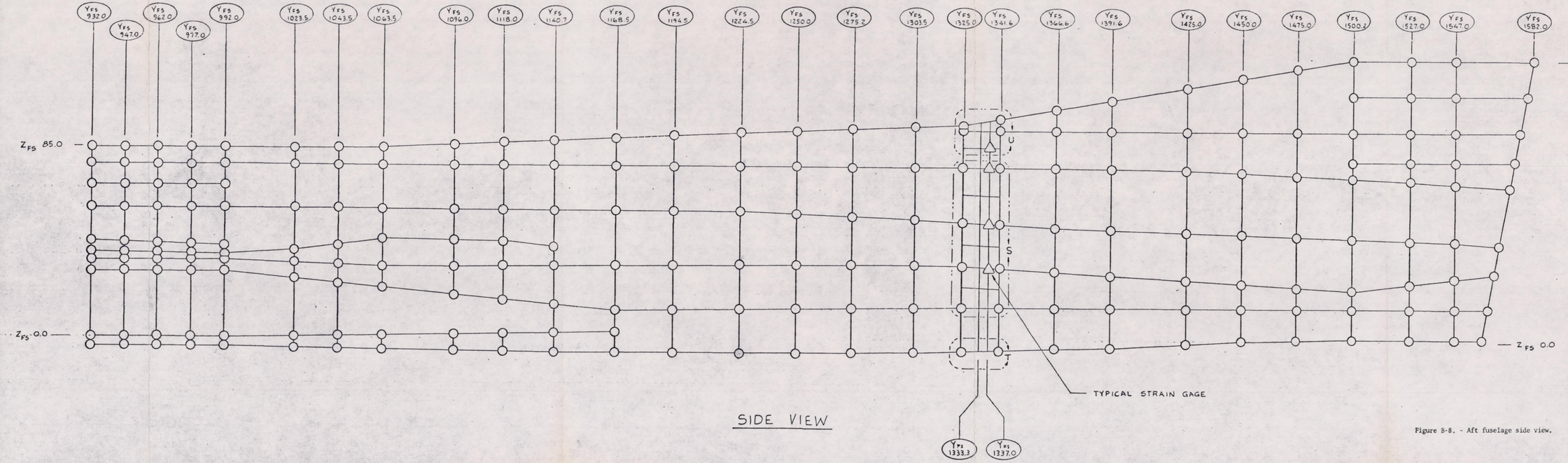

SIDE VIEW

AIRLOADS RESEARCH STUDY	
AFT FUSELAGE SIDE VIEW	
SCALE : 1/20	DATE : 3 FEB. 76
DWN BY : R LATHAM	CHK BY : L SHAH

Z_FS
Y_FS

Figure B-8. - Aft fuselage side view.

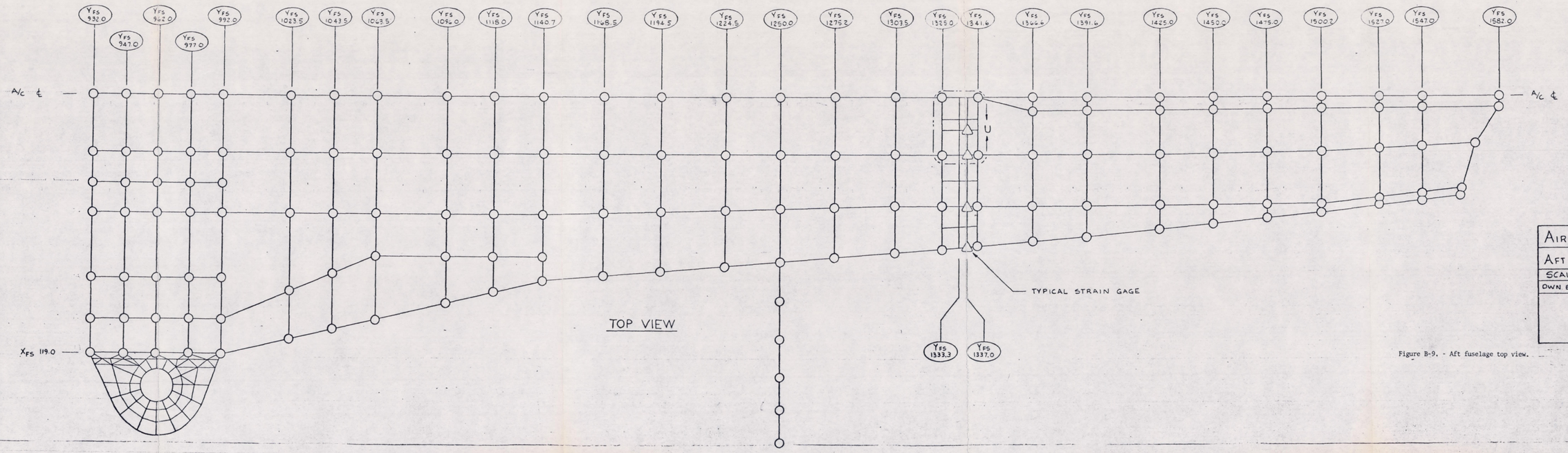

AIRLOADS RESEARCH STUDY	
AFT FUSELAGE TOP VIEW	
SCALE: 1/20	DATE: 3 FEB. 76
DWN BY: R. LATHAM	CHK BY: L. SHAH

YFS
XFS

Figure B-9. - Aft fuselage top view.

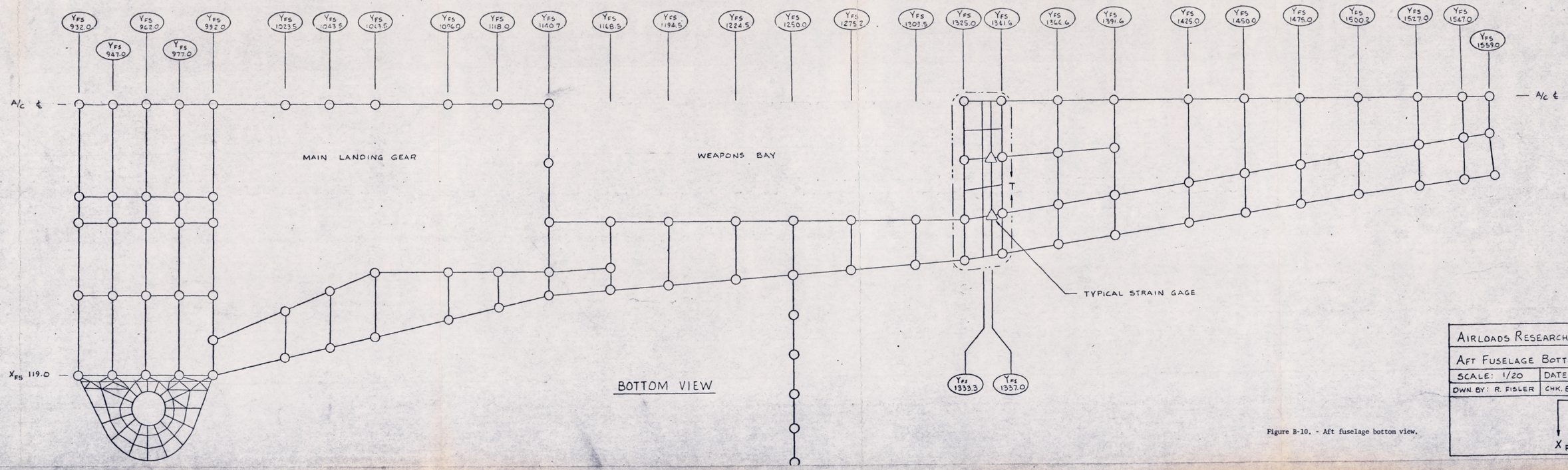

Figure B-10. - Aft fuselage bottom view.

AIRLOADS RESEARCH STUDY	
AFT FUSELAGE BOTTOM VIEW	
SCALE: 1/20	DATE: 3 FEB. 76
DWN. BY: R. FISLER	CHK. BY: R. LATHAM

Y_{FS}

X_{FS}

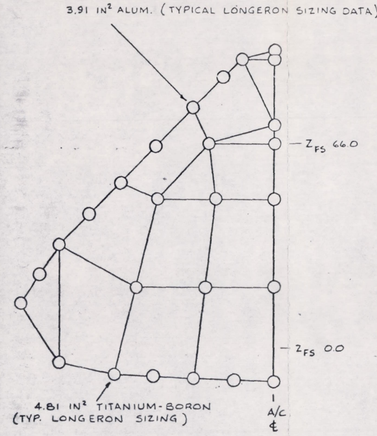

Y_{FS} 1325.0

VIEW LOOKING FORWARD

SCALE: 1/20

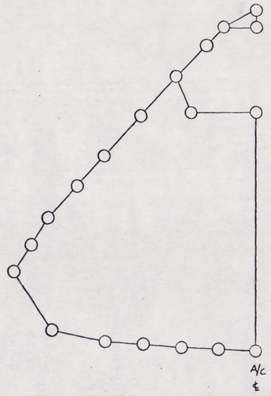

Y_{FS} 1341.6

VIEW LOOKING FORWARD

SCALE: 1/20

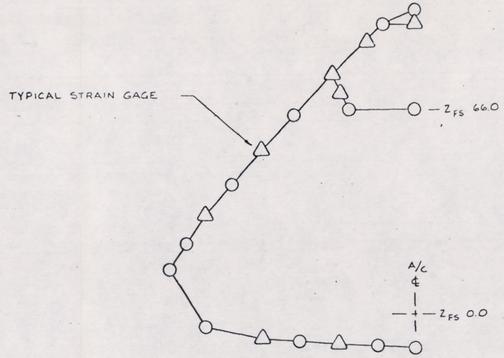

Y_{FS} 1337.0

VIEW LOOKING FORWARD

SCALE: 1/20

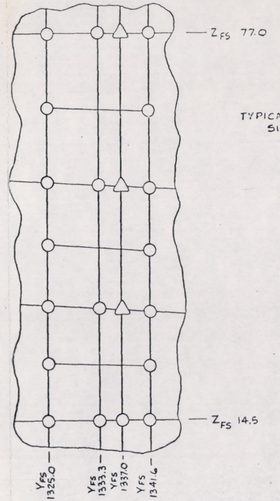

VIEW "S"

SIDE VIEW

SCALE: 1/10

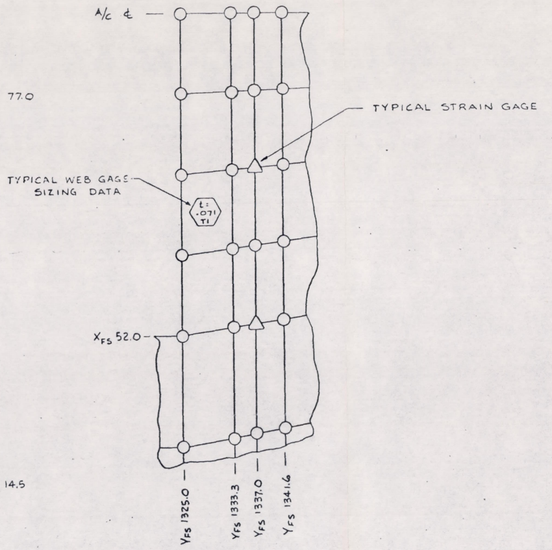

VIEW "T"

BOTTOM VIEW

SCALE: 1/10

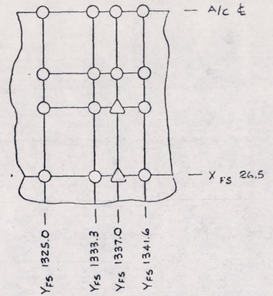

VIEW "U"

TOP VIEW

SCALE: 1/10

AIRLOADS RESEARCH STUDY	
AFT FUSELAGE DETAILS	
SCALE: NOTED	DATE: 3 FEB. 76
DRW. BY: R. LATHAM	CHK BY: L. SHAH

Figure B-11. - Aft fuselage details.

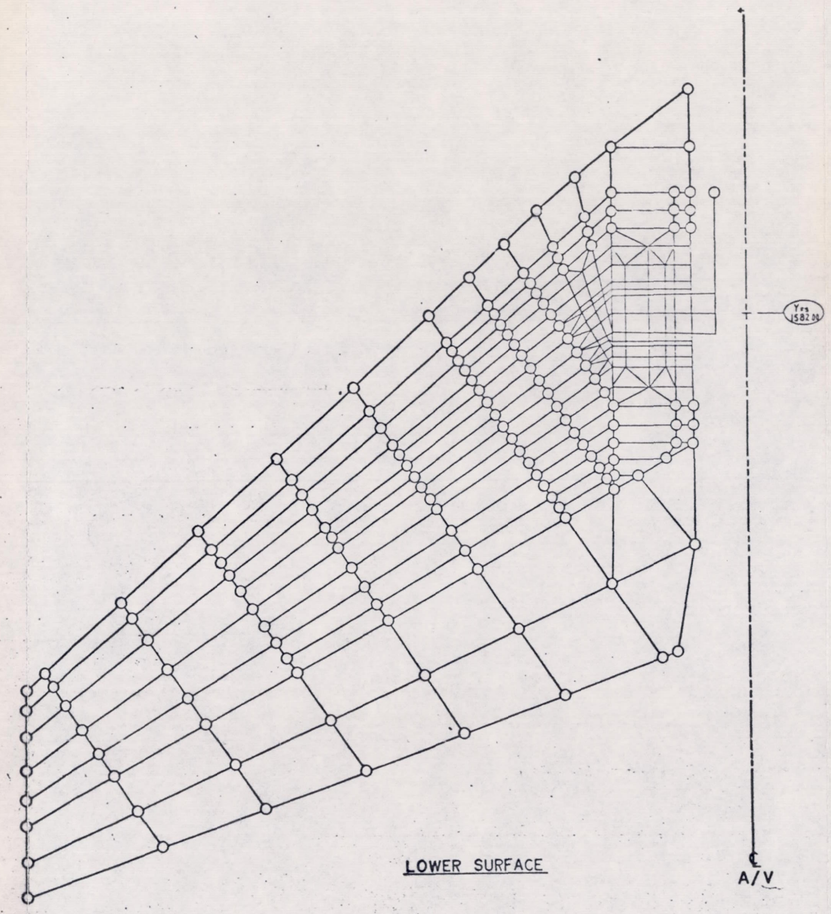

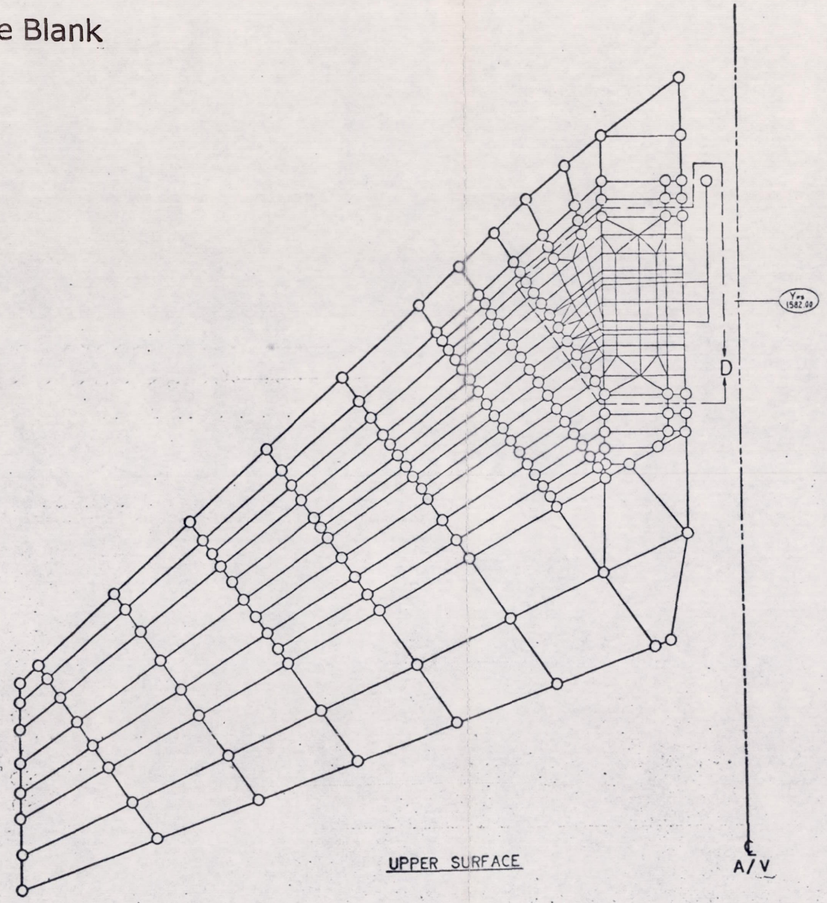

○ – GRID POINT LOCATION

△ – GRID POINT AT STRAIN GAGE LOCATION

ARS	
HORIZONTAL STABILIZER	
SCALE: 1/40 & NOTED	DATE 2-3-76

X_{FS} (OUTB'D)

Y_{FS} (AFT)

Figure B-12. - Horizontal stabilizer.

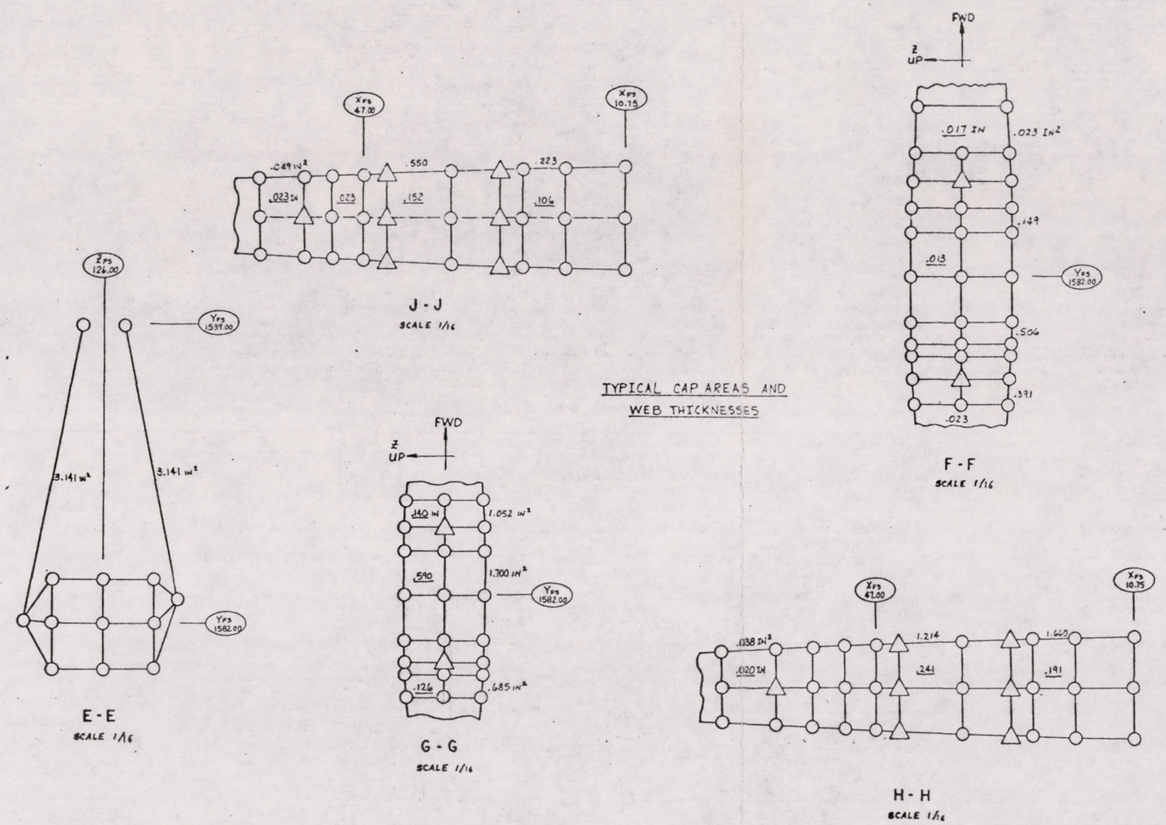

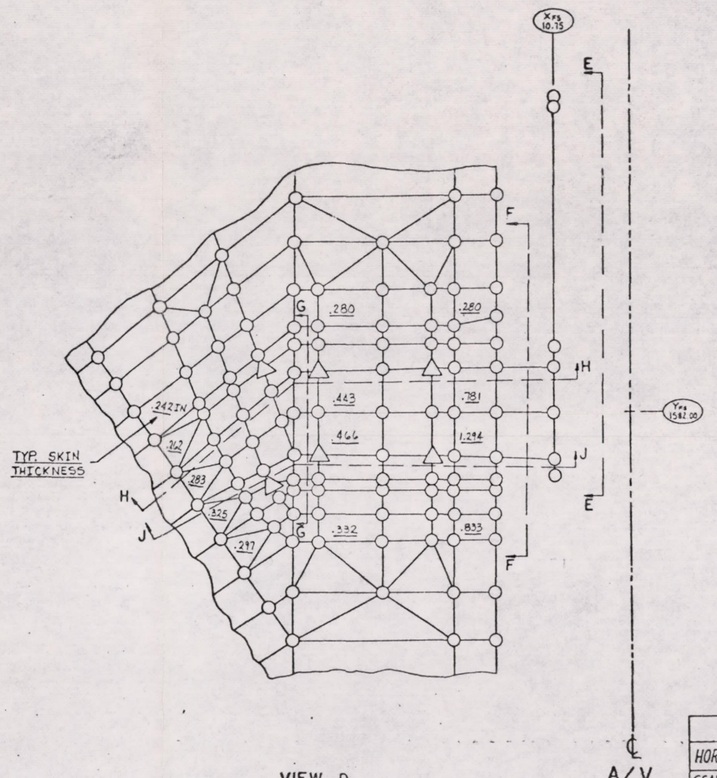

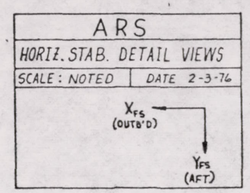

Figure B-13. - Horizontal stabilizer detail views.

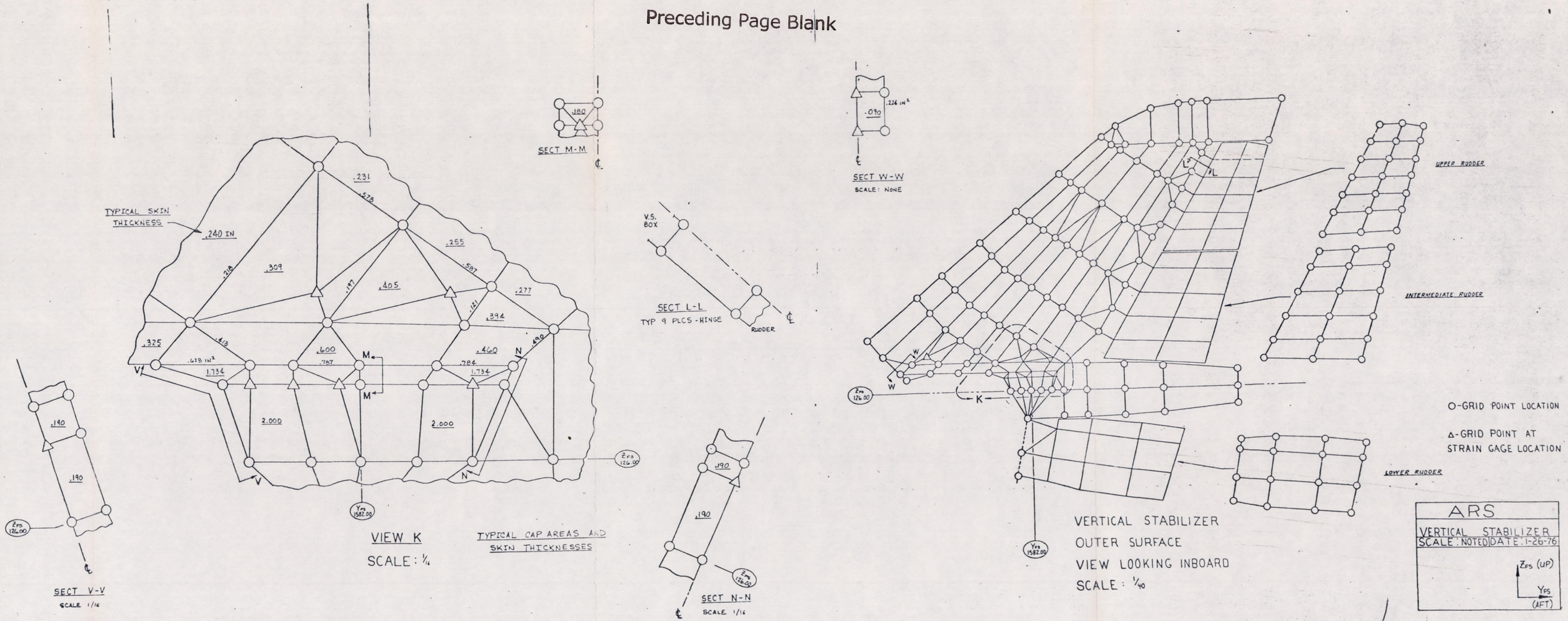

Figure B-14. - Vertical stabilizer.

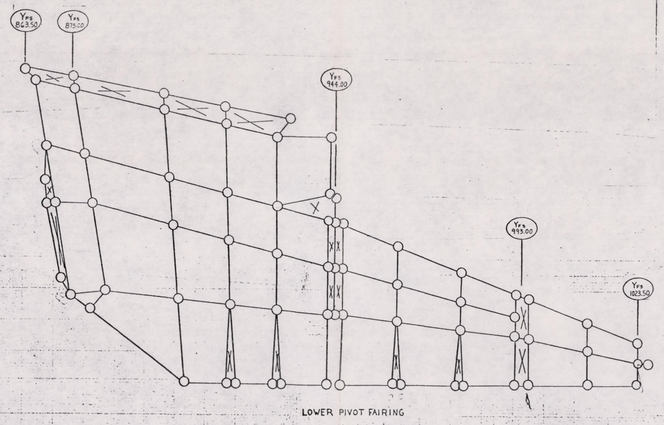

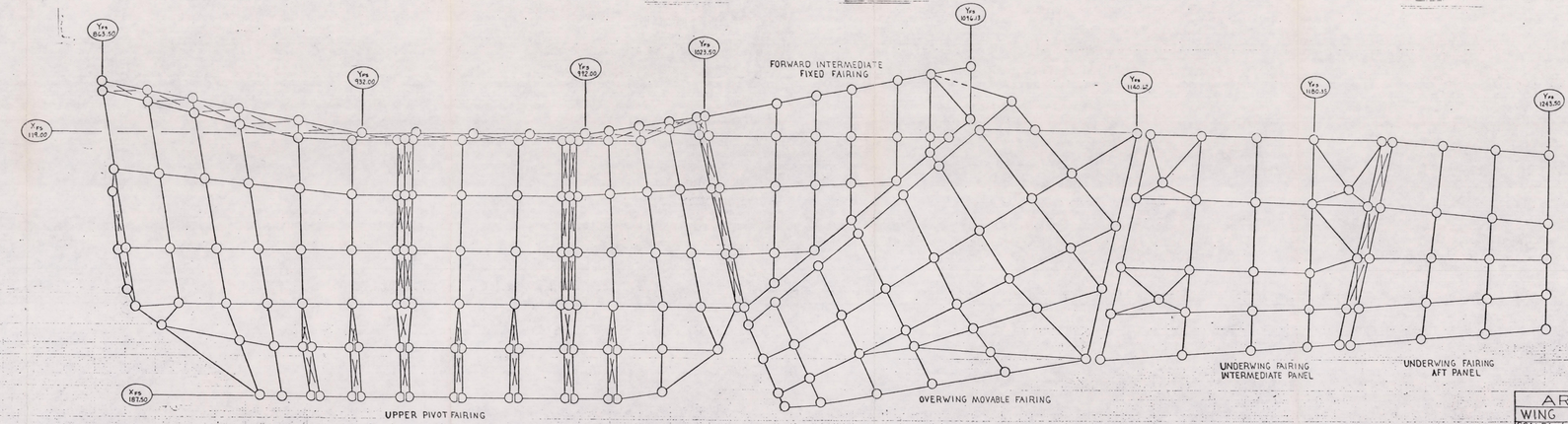

ARS
WING FAIRINGS
SCALE: 1/4 DATE: 1-26-76

Y_{FS} (AFT)
X_{FS} (OUTBD)

Figure B-15. - Wing fairings.

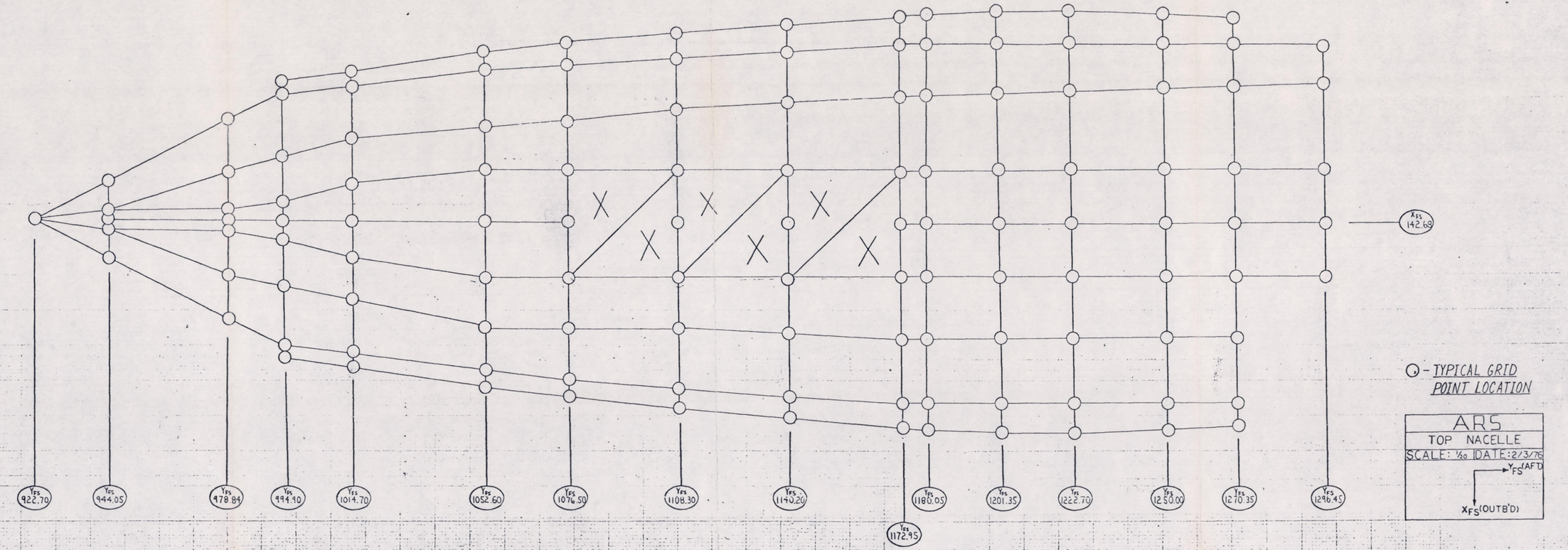

Figure B-16. - Top nacelle.

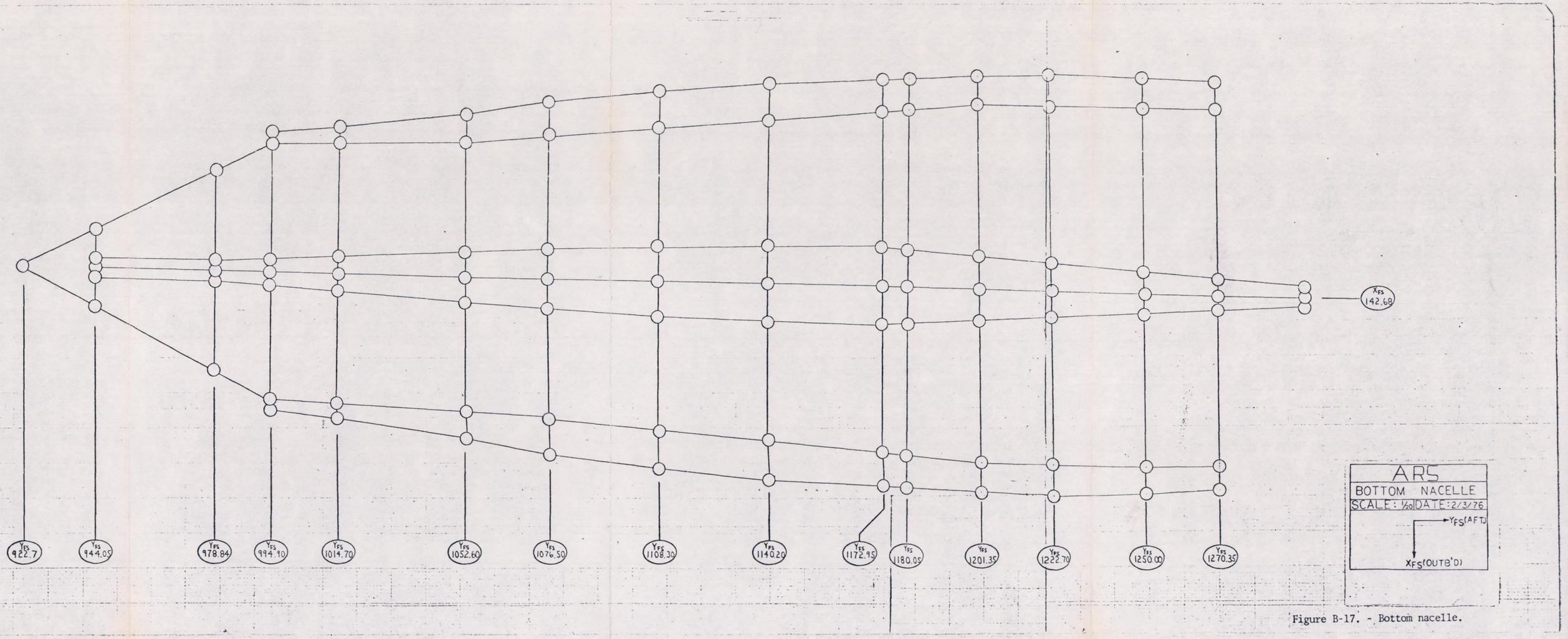

Figure B-17. - Bottom nacelle.

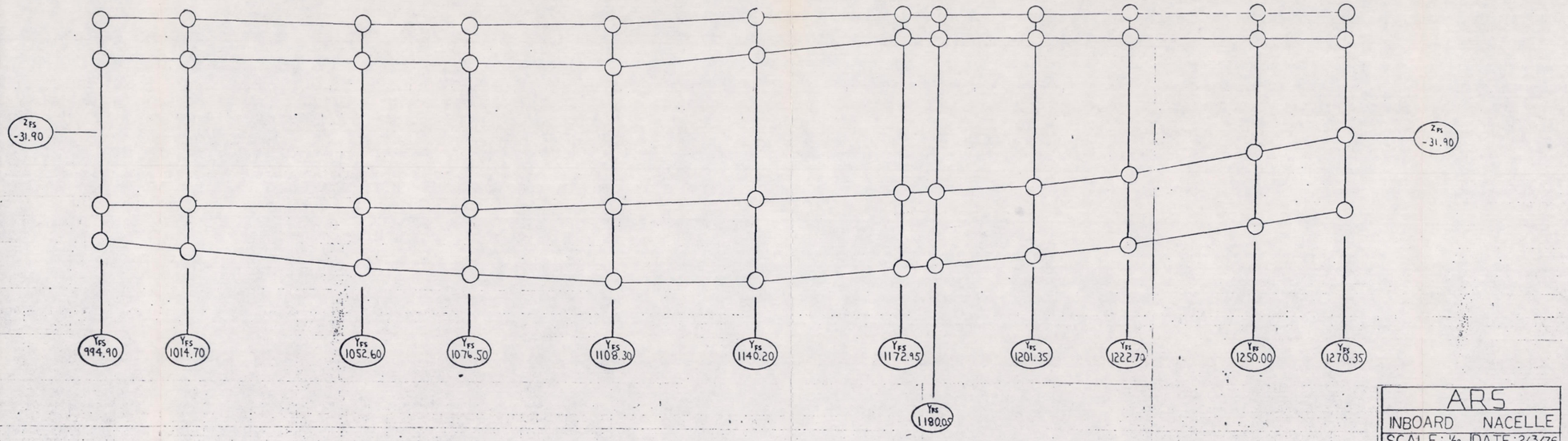

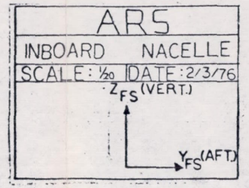

Figure B-18. - Inboard nacelle.

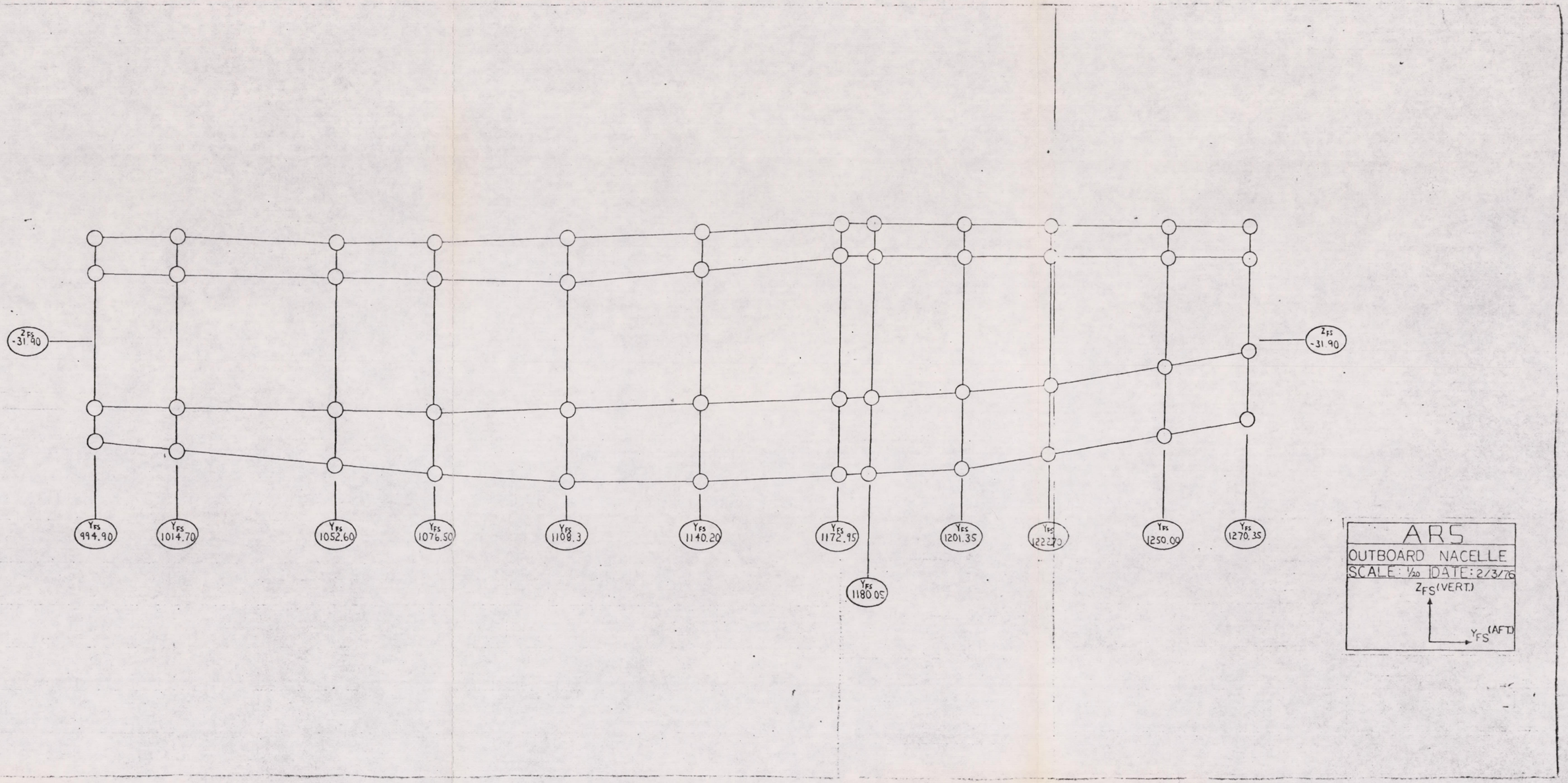

Figure B-19. - Outboard nacelle.

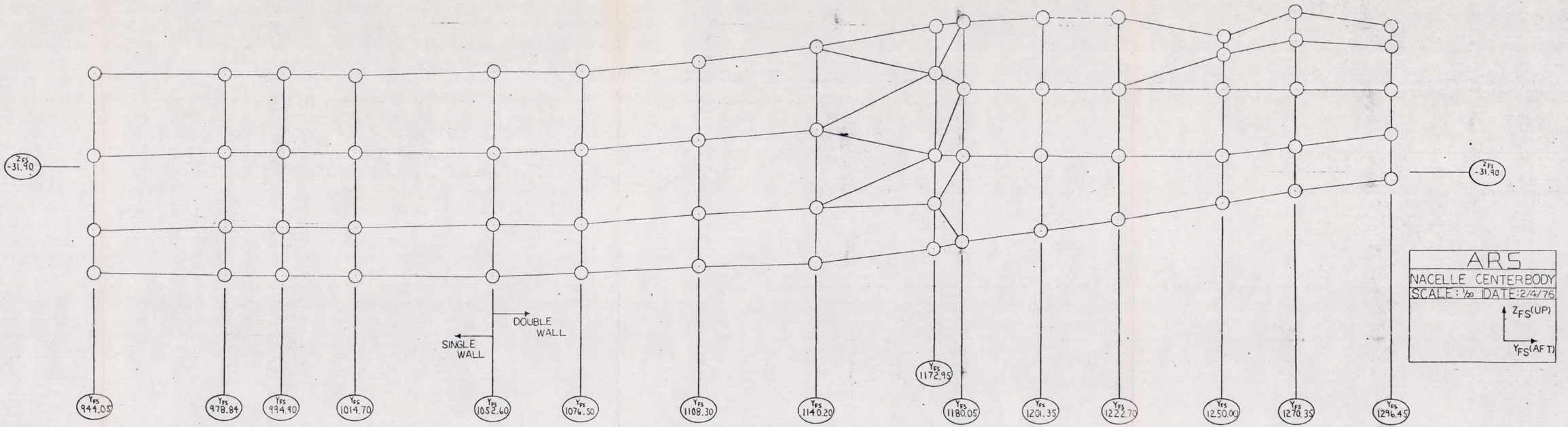

Figure B-20. - Nacelle centerbody.

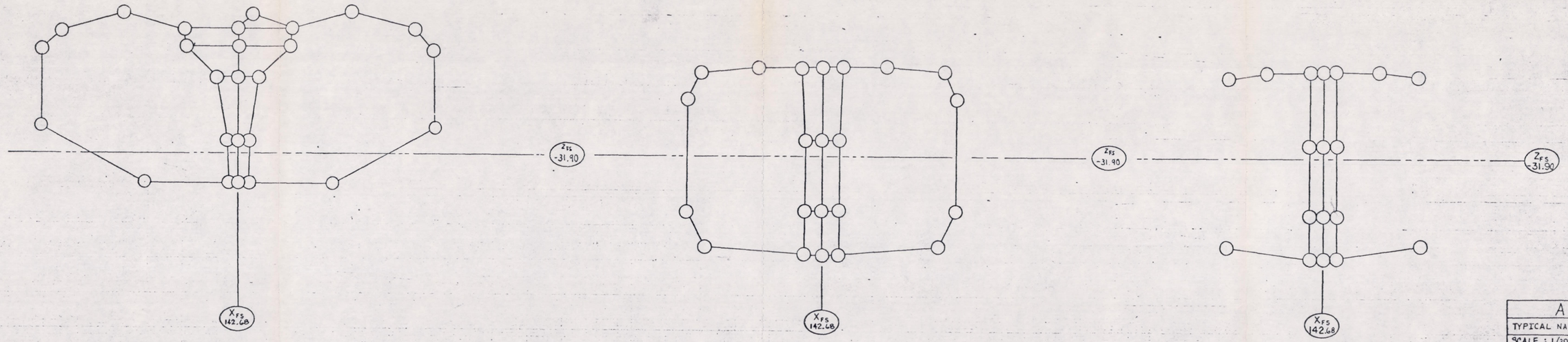

Figure B-21. - Typical nacelle frames.

REFERENCES

(1) The NASTRAN User's Manual (Level 16.0), NASA Report SP-222(03), National Aeronautics and Space Administration, Wash. D.C., March 1976.

(2) The NASTRAN Theoretical Manual (Level 16.0), NASA Report SP-221(03), National Aeronautics and Space Administration, Wash. D.C., March 1976.

(3) Guyan, R.J., "Reduction of Stiffness and Mass Matrices," AIAA Journal, Vol 3, No. 2, February 1965.

1. Report No.	2. Government Accession No.	3. Recipient's Catalog No.
NASA CR-170392		

4. Title and Subtitle	5. Report Date
NASTRAN Model of a Large Flexible Swing-Wing Bomber. Volume I: NASTRAN Model Plans	September 1982
	6. Performing Organization Code

7. Author(s)	8. Performing Organization Report No.
W. D. Mock	NA-76-469
	10. Work Unit No.

9. Performing Organization Name and Address	11. Contract or Grant No.
Rockwell International Los Angeles Division International Airport Los Angeles, CA 90009	NAS4-2308
	13. Type of Report and Period Covered
12. Sponsoring Agency Name and Address	Contractor Report—Final
National Aeronautics and Space Administration Washington, D.C. 20546	14. Sponsoring Agency Code RTOP 505-33-54

15. Supplementary Notes

NASA Technical Monitor: Lawrence S. Schuster, Ames Research Center, Dryden Flight Research Facility

16. Abstract

This report describes the planning, development, and validation of the NASTRAN models of the B-1 aircraft No. 2 structure. Volume I describes the initial planning of the entire modeling effort. Volumes II to V describe, in detail, the development and validation of component structural models. The report includes applicable engineering drawings, NASTRAN structural model plots, and listings of the NASTRAN bulk data deck for each component structure. Validation is documented by comparisons with results from static structural tests.

The subtitles of the volumes included in this report are as follows:

Volume I. NASTRAN Model Plans
Volume II. NASTRAN Model Development—Horizontal Stabilizer, Vertical Stabilizer, and Nacelle Structures
Volume III. NASTRAN Model Development—Wing Structure
Volume IV. NASTRAN Model Development—Fuselage Structure
Volume V. NASTRAN Model Development—Fairing Structure

17. Key Words (Suggested by Author(s))	18. Distribution Statement
NASTRAN Finite elements Structural modeling	Unclassified-Unlimited STAR category 05

19. Security Classif. (of this report)	20. Security Classif. (of this page)	21. No. of Pages	22. Price*
Unclassified	Unclassified	88	A05

For sale by the National Technical Information Service, Springfield, Virginia 22161